

Exponential quantum speedups in quantum chemistry with linear depth

Oskar Leimkuhler* and K. Birgitta Whaley†

Department of Chemistry, University of California, Berkeley and
Berkeley Quantum Information and Computation Center,
University of California, Berkeley, CA 94720, USA

(Dated: May 20, 2025)

We prove classical simulation hardness, under the generalized $P \neq NP$ conjecture, for quantum circuit families with applications in near-term chemical ground state estimation. The proof exploits a connection to particle number conserving matchgate circuits with fermionic magic state inputs, which are shown to be universal for quantum computation under post-selection, and are therefore not classically simulable in the worst case, in either the strong (multiplicative) or weak (sampling) sense. We apply this result to quantum multi-reference methods designed for near-term hardware by ruling out certain dequantization strategies for computing the off-diagonal matrix elements. We demonstrate these quantum speedups for two choices of reference state that incorporate both static and dynamic correlations to model the electronic eigenstates of molecular systems: orbital-rotated matrix product states, which are preparable in linear depth, and generalized unitary coupled-cluster with single and double excitations, for which computing the off-diagonal matrix elements is BQP-complete for any polynomial depth. In each case we discuss the implications for achieving exponential quantum advantage in quantum chemistry on near-term hardware.

I. INTRODUCTION

This article addresses a missing link in the literature on near-term quantum computing. On the one hand, polynomial-depth quantum circuit families such as instantaneous quantum polynomial (IQP) circuits [1, 2], random circuits [3, 4], and graph states [5], have proven quantum speedups in the simulation complexity but lack immediate practical applications. On the other hand, near-term algorithms to prepare quantum chemical ground states, one of the most anticipated industrial and scientific applications for quantum computers, have relied on algorithmic quantum advantage arguments [6–8], meaning there is no known classical algorithm to perform the same task efficiently. This is in contrast to a complexity theoretic quantum speedup, which would guarantee that no such classical algorithm could exist *in principle*, under simple assumptions. The widely adopted unitary coupled-cluster ansatz with single and double excitations (UCCSD) [9, 10] has not previously been shown to provide a complexity theoretic speedup under conservation of particle number (PN), a constraint which is needed to accurately describe the electronic structure of closed molecular systems. Furthermore, related ansätze require circuits of super-linear depth in the system size [11], limiting their practical implementation in the near term. This raises the question: does there exist an efficient near-term algorithm for quantum chemical ground states, with circuit depth that scales linearly in the system size, that also has a provable quantum speedup in the simulation complexity?

In this work we resolve this question in two stages. First, we prove our main technical result, which guar-

antees a worst case exponential separation between the quantum and classical simulation complexity of orbital rotation circuits with four-qubit entangled input states. An orbital rotation is a PN conserving transformation of the fermionic tensor product space, which is mapped under the Jordan-Wigner transformation to a family of efficiently simulable quantum circuits known as matchgates [12–14]. These orbital rotation circuits can be factorized into linear depth [15, 16], suggestive of this being a lower bound for performing useful tasks in electronic structure. It has been shown that generic matchgate circuits with four-qubit magic state inputs are universal under post-selection and are therefore classically hard to simulate unless the polynomial hierarchy collapses [17, 18]. In this work, we extend this analysis to the subset of matchgates which conserve PN, thus implementing a quantum chemical orbital rotation with a fixed number of electrons. Our proof of universality under post-selection implies GapP-hardness of closed simulation up to a constant multiplicative factor, as well as worst case hardness of classical sampling, under the widely held complexity theoretic assumption that the polynomial hierarchy does not collapse [2, 19, 20]. This improves on previous results from fermionic linear optics demonstrating #P-hardness of closed simulation of PN conserving matchgate circuits with magic state inputs up to exact precision [21] or up to an exponentially small additive error [22]. Ref. 22 also proved a worst-to-average case reduction for these weaker results, as well as an anti-concentration property in the output probabilities. By conjecturing that the average case hardness of closed simulation should hold up to a multiplicative factor, Ref. 22 then argued that classical sampling up to a constant additive error is intractable due to a reduction based on Stockmeyer’s theorem [19, 23, 24]. Our result now strengthens this argument by proving the multiplicative hardness conjecture for a worst case instance.

* ol22@berkeley.edu

† whaley@berkeley.edu

We also prove BQP-completeness of closed simulation up to a constant additive error for a more general class of quantum chemistry circuits, consisting of single and double excitation gates with polynomial depth in the system size.

In the second part, we apply our proof of simulation hardness to quantum multi-reference methods for chemical ground state estimation [7, 8, 25, 26], which perform a classical diagonalization of the Hamiltonian (energy) operator in a subspace of low-depth reference states that are expressed in different orbital bases. Our result rules out both efficient computation of the off-diagonal Hamiltonian and overlap matrix elements up to a multiplicative factor by any classical method, and dequantization up to an additive error approximation by mid-circuit ℓ^2 -norm sampling [27], under reasonable assumptions. We explicitly demonstrate this robustness against dequantization for two classes of reference states. The first of these is matrix product states (MPS) in rotated orbital bases, which are prepared by quantum circuits of linear depth in the system size [8]. A linear combination of these reference states provides the ansatz for our recently developed tensor network quantum eigensolver (TNQE) [8], which extends the density matrix renormalization group (DMRG) [28] optimization routine beyond the typical constraint of one-dimensional area law entanglement, and has achieved significantly more accurate and resource-efficient ground state energy estimates than a single-reference UCCSD benchmark in preliminary tests on small molecules. The second class of reference states are represented by UCCD or related UCC correlators acting on rotated Slater determinants, which in linear combination provide the ansatz for the non-orthogonal quantum eigensolver (NOQE) [7]. We present these results as evidence that super-polynomial quantum advantage in quantum chemistry is theoretically achievable using methods suitable for near-term hardware, noting that both of these ansatz classes are designed to compactly represent energy eigenstates of systems characterized by a combination of static and dynamic electron correlation.

II. MAIN RESULTS

Our first technical result is to prove the following theorem:

Theorem 1 (Informal) *The family of orbital rotation circuits \hat{G} with four-qubit fermionic magic state inputs is universal for quantum computation under post-selection.*

From this follow two simulation hardness results:

Corollary 1 (Informal) *Computing the output probabilities of \hat{G} with magic state inputs up to a constant multiplicative factor is GapP-hard.*

Corollary 2 (Informal) *If \hat{G} with magic state inputs can be efficiently sampled in the computational basis by a randomized classical algorithm, then the polynomial hierarchy collapses to the third level.*

We then extend the analysis to a more general class of universal quantum chemistry circuits:

Theorem 2 (Informal) *The family of PN conserving fermionic circuits $\hat{\mathcal{U}}$ consisting of single and double excitation gates is universal for quantum computation.*

This implies a further hardness result for quantum chemistry circuits of any polynomial depth:

Corollary 3 (Informal) *For $\hat{\mathcal{U}}$ of polynomial depth in the number of qubits, computing the output probabilities up to a constant additive error is BQP-complete.*

Definitions for all of the terms in Theorems 1 and 2 and Corollaries 1, 2, and 3 are given in Section III, and their formal statements and proofs are given in Section IV. A consequence of these proofs which may be of independent interest is that nearest-neighbor Givens and phase rotations plus controlled-Z gates are a universal gate set for quantum chemistry.

The Corollaries 1 and 2 can be used to demonstrate worst case quantum speedups in the simulation complexity of any quantum ansatz which is sufficiently expressive to encode any instance of \hat{G} with four-qubit magic state inputs. This has broad implications for the complexity of quantum chemical simulations, given the importance of orbital rotations in electronic structure methods. We show how these results apply to the off-diagonal matrix element computations in quantum multi-reference methods with orbital-rotated MPS or UCCD reference states in Section V.

III. PRELIMINARIES

This article draws on concepts which are known by various names across the disciplines of chemistry, physics, and computer science. Here we lay out the terms and definitions that we will use in the rest of the paper for the benefit of readers from each research field.

A. Quantum circuit simulation

Let $|x\rangle, |y\rangle$ denote arbitrary computational basis states of a register of n qubits. Let \hat{U} denote a family of polynomial size quantum circuits, by which we mean that \hat{U}

could be any quantum circuit of $\text{poly}(n)$ gates on n qubits satisfying some particular rules of construction. For example, \hat{U} might have a restriction on the allowed types of quantum gates, or on the connectivity of the qubits. Let $|\psi\rangle$ denote the corresponding family of quantum states, defined by $|\psi\rangle = \hat{U}|\psi\rangle$. *Closed simulation* refers to the computation of an output probability

$$P = |\langle y|\psi\rangle|^2 = |\langle y|\hat{U}|x\rangle|^2. \quad (1)$$

While exact closed simulation implies that arbitrarily many digits of precision may be obtained, typically one of two notions of approximate closed simulation are considered. Closed simulation up to a *multiplicative factor* refers to the computation of approximate probabilities \tilde{P} up to some constant factor $c \geq 1$ such that

$$\frac{1}{c}P \leq \tilde{P} \leq cP, \quad (2)$$

while closed simulation up to an *additive error* approximation refers to computing \tilde{P} satisfying

$$|\tilde{P} - P| \leq \epsilon, \quad (3)$$

where ϵ is some positive constant independent of n . Because $P \leq 1$, a multiplicative approximation is typically much harder to compute than an additive one (for example, Eq. 2 would be exact whenever $P = 0$). While the term *strong simulation* is often used interchangeably with closed simulation, we will use it to refer specifically to multiplicative approximation (Eq. 2). We will say that a circuit family is efficiently strongly simulable if there exists a classical algorithm to compute P up to a multiplicative factor, for all \hat{U} of $\text{poly}(n)$ gates on n qubits, with $\text{poly}(n)$ time and memory requirements.

Note that a quantum computer does not directly enable strong simulation of \hat{U} . Instead, a quantum register prepared in the state $|\psi\rangle$ allows computational basis vectors $|y\rangle$ to be sampled from the probability distribution,

$$|y\rangle \sim P(y), \quad P(y) \equiv |\langle y|\psi\rangle|^2, \quad (4)$$

by collapsing the superposition under measurement (we will sometimes use $|y\rangle \sim |\psi\rangle$ as short-hand for Eq. 4). This is known as *weak simulation*, and a quantum circuit family is said to be efficiently weakly simulable if there exists a randomized classical algorithm that samples in the computational basis with probabilities according to Eq. 4, with $\text{poly}(n)$ time and memory requirements. While an ideal quantum computer would in principle enable efficient sampling from the exact probability distribution, any realistic quantum computer will be subject to gate and measurement errors. The notions of multiplicative or additive error can be applied to sampling from an approximate distribution, $|y\rangle \sim \tilde{P}(y)$, satisfying Eq. 2 or 3. Unless otherwise stated, we shall assume a multiplicative approximation to the probability distribution when discussing weak simulation.

While an additive error approximation of the output probabilities is generally a more realistic standard, it

is typically much easier to prove simulation hardness up to a multiplicative factor, which does not imply the former. For example, suppose that $|\langle y|\hat{U}|x\rangle|^2$ is not strongly simulable according to Eq. 2, but can be factorized into a pair of unitaries $\hat{U} = \hat{U}_a\hat{U}_b$ which are efficiently simulable. It was demonstrated in Ref. 27 that if one can efficiently sample computational basis states $|z\rangle \sim \hat{U}_b|x\rangle$, and efficiently compute the overlaps $\langle y|\hat{U}_a|z\rangle$ and $\langle z|\hat{U}_b|x\rangle$, then one can efficiently obtain an additive approximation to $|\langle y|\hat{U}|x\rangle|^2$ (see Appendix D). We will refer to this dequantization scheme as *mid-circuit ℓ^2 -norm sampling*. In general, the availability of a factorization of \hat{U} into a pair of efficiently simulable circuits is not typical of unitary transformations, so this particular scheme only applies to circuit families with special structure.

B. Complexity classes

We now briefly review some complexity classes that are relevant for understanding our results (a comprehensive presentation can be found in Ref. 19). The class of problems which are efficiently solvable by a deterministic classical algorithm in polynomial time is denoted by P , while NP is the class of problems for which a solution, once obtained, can be efficiently verified. It is widely believed that NP contains problems that are not in P , known as the $\text{P} \neq \text{NP}$ conjecture. An *oracle* is an abstract entity which grants query access to the solution for a complete (hardest) problem in a given complexity class; the class of problems that can be solved in A with access to an oracle for a problem in B is written as A^{B} . The *polynomial hierarchy* (PH) is the union of a set of nested complexity classes $\Sigma_0 \subseteq \dots \subseteq \Sigma_{\infty}$, defined recursively by

$$\Sigma_0 = \text{P}, \quad \Sigma_i = \Sigma_{i-1}^{\text{NP}}. \quad (5)$$

For example, $\Sigma_1 = \text{NP}$ and $\Sigma_2 = \text{NP}^{\text{NP}}$. A collapse of the polynomial hierarchy to the i 'th level means that $\Sigma_i = \Sigma_{i+1} = \dots = \Sigma_{\infty}$. It is widely conjectured that the polynomial hierarchy does not collapse to *any* finite level, known as the generalized $\text{P} \neq \text{NP}$ conjecture.

The complexity classes $\#\text{P} \subseteq \text{GapP}$ are related to counting the number of solutions to an NP problem. Broadly speaking, $\#\text{P}$ involves summation over exponentially many non-negative terms $\in \{1, 0\}$, each of which is efficiently computed by a classical algorithm, while GapP involves summation over terms which can be positive or negative ($\in \{1, -1\}$), also known as the closure of $\#\text{P}$ under subtraction. These complexity classes are equivalent under *polynomial-time reductions*, meaning that $\text{P}^{\#\text{P}} = \text{P}^{\text{GapP}}$. They contain problems that are thought to be well beyond the capabilities of classical algorithms, evidenced by Toda's theorem [29]:

$$\text{PH} \subset \text{P}^{\#\text{P}}. \quad (6)$$

The class of problems that can be efficiently solved by a *randomized* (probabilistic) classical algorithm with success probability $> 1/2$ is denoted PP . This means there exists an efficient classical algorithm that fails less than half the time. This is a very broad class of problems, as seen by its equivalence to $\#\text{P}$ under polynomial-time reductions ($\text{P}^{\text{PP}} = \text{P}^{\#\text{P}}$), so by Toda's theorem an oracle for a PP -complete decision problem (i.e., an efficient algorithm which never fails) would enable the efficient solution of any problem in PH . By contrast, BPP is the far more limited class of problems which can be efficiently solved by a randomized classical algorithm with bounded success probability $\geq 2/3$. It is known that $\text{P} \subseteq \text{BPP} \subseteq \Sigma_2$ [30], and it has been conjectured that $\text{P} = \text{BPP}$.

The quantum analogue of BPP is BQP , which is the class of problems efficiently solvable by a quantum computer with two-thirds success probability [31]. For example, computing to an additive approximation the output probabilities of an arbitrary polynomial size quantum circuit is a BQP -complete problem [32]. We will say that a quantum circuit family \hat{U} is *universal* for quantum computation if any logical quantum circuit \hat{W} defined on ν qubits, with $\mu = \text{poly}(\nu)$ two-qubit gates, can be encoded within an instance of \hat{U} defined on a larger register of $n = \text{poly}(\nu, \mu)$ qubits using $\text{poly}(n)$ gates. The output probabilities of \hat{U} then cannot be efficiently approximated up to an additive error by a probabilistic classical algorithm unless $\text{BQP} = \text{BPP}$. Furthermore, exactly computing the output probabilities of \hat{U} is GapP -hard [19] (i.e., at least as hard as any problem in GapP). While $\#\text{P}$ and GapP are equivalent under polynomial-time reductions, the approximation of a $\#\text{P}$ sum up to a multiplicative factor is enabled by Stockmeyer's algorithm in $\text{BPP}^{\text{NP}} \subseteq \Sigma_3$ [23], whereas approximating a GapP sum up to a multiplicative factor is also a GapP -hard problem [19]. This is the basis for quantum speedups in the weak simulation of universal quantum circuits, as an efficient classical sampler would enable a multiplicative approximation of the output probabilities by Stockmeyer's algorithm in Σ_3 [19, 24]. Then, by Toda's theorem, we would have that $\text{PH} \subset \text{P}^{\text{GapP}} \subseteq \Sigma_3$, so the polynomial hierarchy would collapse to the third level.

C. Post-selection

If \hat{U} contains additional restrictions such that it is non-universal, then certain simulation hardness results can still be shown provided it is universal under *post-selection*. This refers to deterministically selecting the outcome of a measurement, the same as projecting the quantum state of the register onto the desired measurement outcome, which may have an arbitrarily small non-zero amplitude, and renormalizing. We will say that a restricted quantum circuit family \hat{U} is universal under post-selection if an arbitrary logical quantum computation \hat{W} defined on ν qubits, with $\mu = \text{poly}(\nu)$ gates,

may be encoded within a larger register of $n = \text{poly}(\nu, \mu)$ qubits using an instance of \hat{U} with $\text{poly}(n)$ gates, by post-selecting on the measurement outcomes of some subset of the qubits. It follows that any computation that could be encoded by post-selecting on \hat{W} could also be encoded by post-selecting on \hat{U} with polynomial overhead. This is sometimes written as $\text{post-}\hat{U} = \text{postBQP}$.

This post-selected complexity class is characterized by

$$\text{postBQP} = \text{PP}, \quad (7)$$

which was proven by Aaronson [33]. Together with Toda's theorem (Eq. 6), this implies that $\text{PH} \subset \text{P}^{\text{PP}} = \text{P}^{\text{postBQP}}$, so an efficiently computable solution to any problem in postBQP would imply the same for any problem in PH . In Ref. 20 it was shown that, given $\text{post-}\hat{U} = \text{postBQP}$, an efficient strong simulation of \hat{U} by a deterministic classical algorithm would mean postBQP is efficiently computable in polynomial time, thus the polynomial hierarchy collapses completely ($\text{P} = \text{PH}$, implying $\text{P} = \text{NP}$). If this deterministic classical algorithm were to be replaced by a randomized one, then at the very least $\text{PH} \subset \text{BPP} \subseteq \Sigma_2$. Equivalently, the argument in Ref. 20 implies that the strong simulation of \hat{U} up to a small multiplicative factor is GapP -hard. Furthermore, it was previously shown in Ref. 2 that an efficient weak simulation of \hat{U} would imply $\text{postBQP} = \text{postBPP}$. It is known that $\text{P}^{\text{postBPP}}$ is contained in the third level of the polynomial hierarchy [34], so if \hat{U} were weakly simulable by an efficient classical algorithm it would follow that $\text{PH} \subset \text{P}^{\text{postBPP}} \subseteq \Sigma_3$, i.e., the polynomial hierarchy would collapse to the third level. We summarize these results in the following lemmas, the proofs of which are contained in Refs. 20 and 2 respectively.

Lemma 1 (Fujii and Morimae [20]) *If \hat{U} is universal under post-selection, then the strong simulation of \hat{U} up to a multiplicative factor $1 \leq c < \sqrt{2}$ is GapP -hard. If \hat{U} is efficiently strongly simulable by a deterministic classical algorithm then $\text{P} = \text{PH}$, or if by a randomized classical algorithm then $\text{PH} \subset \text{BPP} \subseteq \Sigma_2$.*

Lemma 2 (Bremner, Jozsa, and Shepherd [2]) *If \hat{U} is universal under post-selection, and is efficiently weakly simulable with $1 \leq c < \sqrt{2}$ by a randomized classical algorithm, then $\text{PH} \subset \text{P}^{\text{postBPP}} \subseteq \Sigma_3$.*

While these results were first derived in the context of IQP circuits [1, 2, 20], they hold in general for any quantum circuit family that is universal under post-selection. An alternative proof of the hardness of weak simulation (the equivalent of Lemma 2) was presented in Ref. 24 in the context of boson sampling. This argument, based on Stockmeyer's algorithm [23], follows directly from Lemma 1, and is similar to that which applies to sampling from universal circuits. For a comprehensive review of these arguments see Ref. 19.

D. Orbital rotations

Electronic structure in second quantization is formalized within a Fock space defined over a finite set of n orthonormal single-particle basis functions, known as *molecular orbitals* or MOs [35] (see Appendix F). The many-body basis states of the Fock space are the computational basis vectors $|x\rangle = |x_1 \dots x_n\rangle$, where $x_p \in \{0, 1\}$ denotes the electron occupancy number of MO p . Each computational basis vector corresponds to an antisymmetrized separable wavefunction known as a Slater determinant, constructed so as to incur a phase of -1 under particle exchange. Operators in the Fock space are spanned by products of creation and annihilation operators which satisfy the fermionic anticommutation relations,

$$\{\hat{a}_p, \hat{a}_q\}_+ = 0, \quad \{\hat{a}_p^\dagger, \hat{a}_q\}_+ = \delta_{pq}, \quad (8)$$

where $\{\cdot, \cdot\}_+$ denotes the anticommutator. Conservation of particle (electron) number, η , is necessary to accurately describe the physical states of an isolated molecular system. Under this restriction, any physically allowed quantum state must reside within the block of $\binom{n}{\eta}$ Slater determinants which span the PN conserving subspace. The size of this subspace grows exponentially when n and η are increased in proportion. In addition, any physical observable or transformation operator must have an expansion in terms of equal combinations of annihilation and creation operators. For example, the electronic structure Hamiltonian is given by

$$\hat{H} = \sum_{pq}^n h_{pq} \hat{a}_p^\dagger \hat{a}_q + \sum_{pqrs}^n h_{pqrs} \hat{a}_p^\dagger \hat{a}_q^\dagger \hat{a}_r \hat{a}_s. \quad (9)$$

The mathematical object of central importance in our study is an *orbital rotation*, which is a unitary transformation of the MOs, characterized by an $n \times n$ unitary coefficient matrix \mathbf{G} (with elements g_{pq}). We will use the symbol \hat{G} for the corresponding Fock space operator, which can be understood in terms of its action on the fermionic creation and annihilation operators,

$$\hat{G} \hat{a}_p \hat{G}^\dagger = \sum_{q=1}^n g_{pq} \hat{a}_q. \quad (10)$$

This represents a subset of the more general class of Bogoliubov transformations, which transform between any pair of fermionic Gaussian states [36]. Under conserved PN, Eq. 10 provides an analogous transformation between any pair of Slater determinants in rotated orbitals, forming a subgroup of unitary operators in the Fock space (any product of rotations $\hat{G}_a \hat{G}_b$ is also an orbital rotation, and every \hat{G} has a unique inverse rotation \hat{G}^\dagger).

A Slater determinant describes the wavefunction of uncorrelated electrons, so a time evolution operator that does not include two-body or higher interactions must

transform to another Slater determinant. Thus the orbital rotation in Eq. 10 is related to unitary evolution under a one-body (quadratic) Hamiltonian describing non-interacting fermions. In second quantization this correspondence manifests in the Thouless theorem [37], which may be stated as

$$\hat{G} = \exp \left(\sum_{pq}^n \tilde{g}_{pq} (\hat{a}_p^\dagger \hat{a}_q - \hat{a}_q^\dagger \hat{a}_p) \right), \quad (11)$$

where \tilde{g}_{pq} are matrix elements of $\tilde{\mathbf{G}} = \ln(\mathbf{G})$. The overlap between two η -particle Slater determinants $|x\rangle$ and $|y\rangle$ expressed in rotated orbitals is classically efficiently computable, and is given by

$$\langle y | \hat{G} | x \rangle = \det(\bar{\mathbf{G}}_{xy}), \quad (12)$$

where $\bar{\mathbf{G}}_{xy}$ is the $\eta \times \eta$ submatrix obtained by selecting the rows and columns of \mathbf{G} according to the occupied modes in $|x\rangle$ and $|y\rangle$ respectively [13].

E. Matchgates

The Jordan-Wigner (JW) transformation [38] provides a direct mapping between the Fock space vectors and the computational basis states of a qubit register. Under this mapping the fermion operators are expressed in terms of the Pauli X , Y , and Z gates as

$$\hat{a}_p \mapsto (X_p - iY_p)Z_{p-1} \cdots Z_1, \quad (13)$$

where X_p denotes an X gate applied on qubit p , etc., and we have dropped the hat notation for one- and two-qubit gates. The Z gates on qubits $1, \dots, p-1$, known as JW strings, are necessary to preserve the fermionic anticommutation relations (Eqs. 8). This construction defines an ordering of the qubits along one dimension from $p = 1, \dots, n$. We can then define *nearest-neighbor* gates as those that act only between pairs of qubits p and $p+1$.

Under the JW transformation, non-interacting fermion evolution is mapped onto a restricted quantum circuit family known as *matchgates*, first proposed by Valiant [12], before the connection to fermionic systems was established [13, 39]. Matchgate circuits consist exclusively of nearest-neighbor two-qubit gates that are elements of the matchgate set $\{\mathcal{G}\}$, defined in terms of a pair of 2×2 unitary matrices \mathbf{u}, \mathbf{v} as

$$\mathcal{G} = \begin{pmatrix} u_{11} & 0 & 0 & u_{12} \\ 0 & v_{11} & v_{12} & 0 \\ 0 & v_{21} & v_{22} & 0 \\ u_{21} & 0 & 0 & u_{22} \end{pmatrix}, \quad \det(\mathbf{u}) = \det(\mathbf{v}). \quad (14)$$

Under PN conservation we impose the additional restriction that \mathbf{u} is diagonal, i.e., $u_{12} = u_{21} = 0$. The restriction to nearest-neighbor gates is essential: while matchgate circuits are strongly simulable by a classical algorithm in P , the inclusion of non-nearest neighbor gates,

equivalent to the inclusion of the SWAP gate into the gate set, enables universal quantum computation [14] (GapP-hard). In order to satisfy the matchgate definition (Eqs. 14) one must instead use the fermionic SWAP (FSWAP) gate $F \in \{\mathcal{G}\}$, which flips the sign of the $|11\rangle$ state, simulating fermionic antisymmetry under particle exchange [40],

$$F = \begin{pmatrix} 1 & 0 & 0 & 0 \\ 0 & 0 & 1 & 0 \\ 0 & 1 & 0 & 0 \\ 0 & 0 & 0 & -1 \end{pmatrix}. \quad (15)$$

The FSWAP gate is an example of a PN conserving matchgate. Others include the nearest-neighbor Givens rotation gate $G(\theta)$ and the single-qubit phase gate $R(\varphi)$, which are expressed in terms of fermion operators as

$$G_p(\theta) = \exp(\theta(\hat{a}_p^\dagger \hat{a}_{p+1} - \text{h.c.})), \quad (16)$$

$$R_p(\varphi) = \exp(i\varphi \hat{a}_p^\dagger \hat{a}_p), \quad (17)$$

respectively. Substitution of the JW transformation (Eq. 13) into Eqs. 16 and 17 then yields the two-qubit matchgate representations of $G(\theta)$ and $R(\varphi) \otimes \mathbb{1}$:

$$G(\theta) = \begin{pmatrix} 1 & 0 & 0 & 0 \\ 0 & c & -s & 0 \\ 0 & s & c & 0 \\ 0 & 0 & 0 & 1 \end{pmatrix} \quad \begin{aligned} c &= \cos \theta \\ s &= \sin \theta, \end{aligned} \quad (18)$$

$$R(\varphi) \otimes \mathbb{1} = \begin{pmatrix} 1 & 0 & 0 & 0 \\ 0 & 1 & 0 & 0 \\ 0 & 0 & \alpha & 0 \\ 0 & 0 & 0 & \alpha \end{pmatrix} \quad \alpha = e^{i\varphi}. \quad (19)$$

Note that these gates are localized on qubits p and $p+1$, due to cancellation of the JW strings on the remaining qubits (this would no longer be the case if the transformation in Eq. 16 were applied to non-neighboring qubits).

The strong simulation of PN conserving matchgate circuits can be understood by their equivalence to orbital rotations through Eq. 11, which are efficiently classically simulable by Eq. 12, as demonstrated in Ref. 13. It was later shown in Ref. 15 that a Givens rotation gate on qubits p and $p+1$ (as in Eq. 16) is equivalent to premultiplying the coefficient matrix \mathbf{G} by an $n \times n$ Givens rotation matrix that mixes the p 'th and $(p+1)$ 'th rows and columns. In this manner, a sequence of $\binom{n}{2}$ Givens rotation gates can be used to perform a QR factorization of \mathbf{G} , after which it is in diagonal form. The net effect of this analysis is that any orbital rotation may be factorized into a circuit of $O(n^2)$ matchgates,

$$\hat{G} = \prod_{q=1}^n R_q(\varphi_q) \prod_{k=1}^{\binom{n}{2}} G_{p_k}(\theta_k), \quad (20)$$

where (p_k, θ_k) are pairs of register indices and rotation angles that perform the QR factorization, and the final

layer of phase gates accounts for the diagonal entries. Eq. 20 assumes \mathbf{G} is real-valued, but this can be extended to complex-valued \mathbf{G} using additional phase gates. These operations can be performed in parallel with linear circuit depth in n . We summarize this duality between PN conserving matchgate circuits and orbital rotations, and their factorization into linear depth, in the following lemma, the proof of which is contained in Refs. 13 and 15.

Lemma 3 (From Terhal and DiVincenzo [13] and Kivlichan *et al.* [15]) *Under the JW transformation, any PN conserving matchgate circuit on n qubits implements an orbital rotation \hat{G} , characterized by an $n \times n$ coefficient matrix \mathbf{G} , which may in turn be factorized into a PN conserving matchgate circuit of depth $O(n)$ that implements the same orbital rotation.*

IV. PROOFS OF HARDNESS

In this section we formally re-state and prove our main results (Theorems 1 and 2), with further details in Appendices A and B. The proof of Theorem 1 is inspired by Refs. 14, 17 but extended with a new construction in terms of PN conserving matchgates.

Theorem 1 (Orbital rotations with magic state inputs are universal under post-selection) *The output state of any quantum computation of μ two-qubit gates on ν qubits can be encoded on a register of $n = 2\nu + 12\mu$ qubits prepared in the state $\hat{G}|\Phi\rangle$, where \hat{G} is an orbital rotation circuit under the JW transformation, $|\Phi\rangle = |01\rangle^{\otimes \nu} \otimes |M\rangle^{\otimes 3\mu}$, and $|M\rangle$ is a four-qubit fermionic magic state, by post-selecting on the measurement outcome $|1010\rangle^{\otimes 3\mu}$ of the last 12μ qubits.*

Proof. By Lemma 3, \hat{G} is described by a PN conserving matchgate circuit. Because the computational basis states $|0\rangle$ and $|1\rangle$ encode different occupancy numbers under the Jordan-Wigner transformation, and a particle number conserving unitary is block-diagonal in the different particle number subspaces, an arbitrary quantum computation must be logically encoded within one of the fixed PN subspaces. This can be achieved using a *dual-rail* representation [41, 42], wherein the logical $|0\rangle$ and $|1\rangle$ states are respectively encoded by the $|01\rangle$ and $|10\rangle$ states of a physical qubit pair. In this manner any ν -qubit logical computational basis state can be encoded by a Slater determinant of ν fermions in 2ν orbitals. Any logical single-qubit gate can then be mapped directly to particle number conserving matchgates via its decomposition into Euler angles [31], as illustrated in Figure 1, corresponding to a complex-valued orbital rotation on the dual-rail qubit.

To implement an arbitrary logical computation one gate is required that is not in the PN conserving matchgate set [43]. The nearest-neighbor controlled-Z (CZ) gate is sufficient, since logical single-qubit rotations together with the logical CZ gate form a universal gate

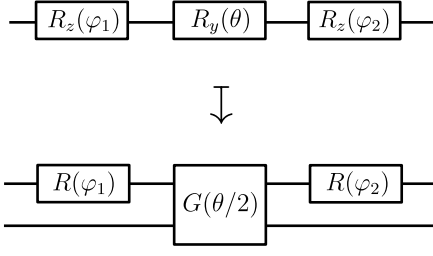


Figure 1. A logical single-qubit gate is decomposed into R_y and R_z rotations via Euler angles $(\varphi_1, \theta, \varphi_2)$ up to a global phase (top). Each logical rotation is mapped to a PN conserving matchgate in the dual-rail encoding (bottom). $G(\theta)$ denotes a Givens rotation gate (Eq. 18) and $R(\varphi) = e^{-i\varphi/2}R_z(\varphi)$ is the generic phase rotation gate (Eq. 19).

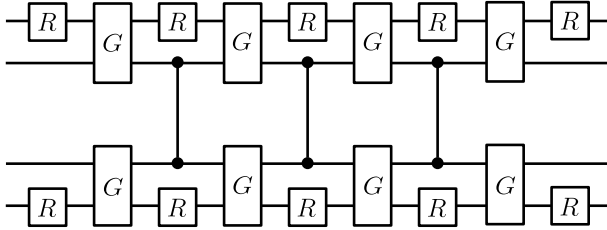


Figure 2. A logical two-qubit gate is implemented in the dual-rail encoding via Givens rotations and phase rotation gates applied locally on each dual-rail qubit, and controlled- Z gates applied between the dual-rail qubits (see Appendix A).

set. In the dual-rail encoding, the logical CZ operation between neighboring dual-rail qubits must flip the sign of the $|10\rangle|10\rangle$ state while leaving the orthogonal subspace unchanged. This is achieved with two physical gates: a Z gate on the third qubit applies a -1 phase to the $|10\rangle|10\rangle$ and $|01\rangle|10\rangle$ states, then a CZ gate between the middle two qubits flips the phase of the $|01\rangle|10\rangle$ state back to $+1$. With this extension of the gate set, an arbitrary logical two-qubit gate can be implemented using the construction in Figure 2. This follows from the decomposition of a logical two-qubit gate into single-qubit rotations and three CNOT gates [44], which are equivalent to CZ gates under Hadamard conjugation (see Appendix A). Logical gates between arbitrarily separated dual-rail qubits may be implemented using nearest-neighbor FSWAP networks (because each dual-rail qubit is always occupied by a single particle, these FSWAP networks incur only a global phase of ± 1 due to fermionic anticommutation). Therefore a logical circuit of μ two-qubit gates, with arbitrary connectivity, can be implemented in the dual-rail encoding using only nearest-neighbor PN conserving matchgates and at most 3μ nearest-neighbor CZ gates.

Figure 3 shows how the CZ gate can be implemented under post-selection using only PN conserving match-

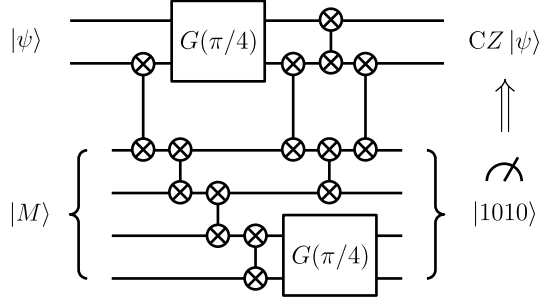


Figure 3. A gadget to implement the controlled- Z gate under post-selection using only Givens rotation gates $G(\pi/4)$ and FSWAP gates (linked crossed circles, Eq. 15), and a magic state $|M\rangle$ as defined in Eq. 21. The CZ gate is implemented on the top two qubits provided that the bottom four qubits are measured in the $|1010\rangle$ state, which occurs with probability $1/4$ (see Appendix B).

gates and a four-qubit, two-particle magic state,

$$|M\rangle = \frac{1}{2}(|1001\rangle - |0110\rangle - |0101\rangle - |1010\rangle) \quad (21)$$

(see Appendix B). This construction is similar to the adaptive measurement gadget in Refs. 17, 18 for the SWAP gate using PN non-conserving matchgates. However, in our construction the CZ is not implemented deterministically; the correct operation is only realized upon obtaining a specific measurement outcome, in this case the $|1010\rangle$ state, which occurs with probability $1/4$. Since the magic state has even particle number it can be moved around the register via FSWAP networks without incurring any net fermionic phase flips. The magic states can therefore be initialized on the last 12μ qubits of the quantum register and transported to the correct positions as needed during the computation using FSWAP networks. The measurement qubits may then be returned to the end of the quantum register by FSWAP networks after each use. Then by measuring the last 12μ qubits and post-selecting on the outcome $|1010\rangle^{\otimes 3\mu}$, which occurs with probability $1/4^{3\mu}$, the desired logical output state is realized on the first 2ν qubits. We have thereby shown that any logical quantum computation of μ two-qubit gates on ν qubits can be obtained under post-selection using a PN-conserving matchgate circuit \hat{G} acting on the input state $|\Phi\rangle = |01\rangle^{\otimes \nu} \otimes |M\rangle^{\otimes 3\mu}$, requiring at most $n = 2\nu + 12\mu$ qubits. \square

A byproduct of this analysis is that nearest-neighbor Givens and phase rotations plus CZ gates are a universal gate set for quantum chemistry, since they are sufficient to implement the controlled single excitation gate of Ref. 42 (see Appendix A). Note that while \hat{G} is a complex-valued orbital rotation in the above statements, the same results can be shown to hold for real-valued orbital rotations with a constant factor more qubits (see Appendix C).

The dual-rail encoding of arbitrary logical gates can also be used to show universality (without requiring post-

selection) for the more general family of quantum chemistry circuits consisting of single (matchgate) and double (two-body) fermionic excitation gates, which we denote $\hat{\mathcal{U}}$, as expressed in the following theorem.

Theorem 2 (Universality of quantum chemistry circuits) *Any logical computation of μ two-qubit gates on ν qubits may be encoded on a register of $n = 2\nu$ qubits by a PN conserving fermionic circuit, $\hat{\mathcal{U}}$, consisting of $\text{poly}(\nu, \mu)$ single and double excitation gates.*

Proof. By the logical two-qubit gate construction in Figure 2, any logical computation of μ two-qubit gates on ν qubits may be realized in the dual-rail encoding on a register of $n = 2\nu$ qubits, using only PN conserving matchgates and 3μ CZ gates. Under the JW transformation, we may write the CZ gate acting between qubits p and q as a double number excitation,

$$\text{CZ} = \exp(i\pi\hat{n}_p\hat{n}_q), \quad (22)$$

where $\hat{n}_p = \hat{a}_p^\dagger\hat{a}_p$. Thus any logical circuit can be encoded by an instance of $\hat{\mathcal{U}}$ with polynomial overhead, therefore $\hat{\mathcal{U}}$ is universal for quantum computation. \square

Theorem 2 extends a previous result, that PN non-conserving fermionic single and double excitation gates are a universal gate set [45], to the case of conserved PN. Theorems 1 and 2, together with Lemmas 1 and 2, prove Corollaries 1, 2, and 3, which we re-state formally below.

Corollary 1 (From Theorem 1 and Lemma 1) *Strong simulation of $\hat{G}|\Phi\rangle$ up to a multiplicative factor $1 \leq c < \sqrt{2}$ is GapP-hard.*

Corollary 2 (From Theorem 1 and Lemma 2) *If $\hat{G}|\Phi\rangle$ is efficiently weakly simulable up to a multiplicative factor $1 \leq c < \sqrt{2}$ by a randomized classical algorithm, then $\text{PH} \subset \text{P}^{\text{postBPP}} \subseteq \Sigma_3$.*

Corollary 3 (From Theorem 2) *Closed simulation of $\hat{\mathcal{U}}$ up to a constant additive error ϵ , where $\hat{\mathcal{U}}$ consists of $\text{poly}(n)$ single and double excitation gates on n qubits, is BQP-complete.*

We make two remarks about Corollaries 1 and 2. First, they are worst case results, meaning that there is at least some instance of \hat{G} for which they hold. Ideally, we should like to extend these results to the *average case*, by which we mean the majority of instances of \hat{G} as characterized by a coefficient matrix \mathbf{G} sampled uniformly according to the Haar measure over the unitary group group $\text{U}(n)$ (we refer to this as a *Haar-random* instance of \hat{G}). Second, as discussed in Section III A, a multiplicative approximation of the output probabilities (Eq. 2) does not correspond to the level of accuracy typically enabled by a quantum computer subject to physical device errors. A more robust version of these results would be expressed in terms of a constant additive approximation to the output probabilities.

Progress toward both the corresponding average case result and weak simulation up to an additive approximation of the output probabilities can be made using the results of Ref. 22, which we now briefly summarize. Let $|\Phi'\rangle = |M\rangle^{\otimes m}$, so that $n = 4m$ and $\eta = 2m$. Then the following theorems hold.

Theorem 3 (Oszmaniec *et al.* [22]; worst-to-average case reduction) *For Haar-random \hat{G} , closed simulation of $\hat{G}|\Phi'\rangle$ to exact precision, or to an exponentially small additive error $\epsilon = \exp[-O(m^6)]$, is $\#\text{P}$ -hard for a fraction of instances $1 - o(m^{-2})$.*

Theorem 4 (Oszmaniec *et al.* [22]; anticoncentration) *For Haar-random \hat{G} , for any computational basis state $|x\rangle$ and any $\delta \in [0, 1]$, we have that $|\langle x|\hat{G}|\Phi'\rangle|^2 > \delta/\binom{n}{\eta}$ with probability greater than $(1 - \delta^2)/5.7$.*

These theorems were proven in Ref. 22, wherein Theorem 3 was used as evidence to support the conjecture that average case $\#\text{P}$ -hardness applies not only for an exponentially small additive error $\epsilon = \exp[-O(m^6)]$, but also for a constant multiplicative factor approximation (as in Corollary 1). Proof of this conjecture, in combination with Theorem 4, would be sufficient to prove that weak simulation of $\hat{G}|\Phi'\rangle$ up to a constant additive error is classically intractable for the average case unless the polynomial hierarchy collapses to the third level [19, 22, 24]. We note that while Ref. 22 conjectured average case $\#\text{P}$ -hardness of strong simulation up to a multiplicative factor, it was not proven therein even for the hardest case. By demonstrating universality under post-selection, we have now provided a proof of hardness for the worst case. Thus our Corollary 1 in the hardest case, as a consequence of our proof of Theorem 1, lends further support to the conjectured average case hardness of strong simulation of $\hat{G}|\Phi'\rangle$ up to a multiplicative factor, and by extension also to the conjectured average case hardness of weak simulation of $\hat{G}|\Phi'\rangle$ up to a constant additive error.

V. QUANTUM MULTI-REFERENCE METHODS

Here we apply Corollaries 1, 2, and 3 to the TNQE and NOQE algorithms [7, 8]. These are hybrid quantum-classical methods designed to address situations with both *static* (strong) and *dynamic* (weak, or perturbative) electronic correlations, for which multi-reference descriptions are needed [46–48] (see Appendix F). In contrast to known classical analogues, they are strictly variational, and can be made size-consistent in the appropriate limit. In each case we discuss the implications for achieving quantum advantage in quantum chemical ground state estimation, under the assumption that the generalized $\text{P} \neq \text{NP}$ conjecture is true.

A. General framework

The idea behind quantum multi-reference methods [7, 8, 25, 26], a variant of quantum subspace methods [49], is to construct a wavefunction ansatz from a linear combination of reference states in different orbital bases,

$$|\psi\rangle = \sum_{i=1}^M c_i \hat{G}_i |\phi_i\rangle, \quad (23)$$

where the \hat{G}_i operators rotate each reference state into a common single-particle basis. Instead of directly preparing $|\psi\rangle$ with a single quantum circuit, a quantum computer is used to evaluate the Hamiltonian and overlap subspace matrices \mathbf{H} and \mathbf{S} , with matrix elements given by

$$h_{ij} = \langle \phi_i | \hat{H}_i \hat{G}_{ij} | \phi_j \rangle, \quad s_{ij} = \langle \phi_i | \hat{G}_{ij} | \phi_j \rangle, \quad (24)$$

where $\hat{G}_{ij} = \hat{G}_i^\dagger \hat{G}_j$ and $\hat{H}_i = \hat{G}_i^\dagger \hat{H} \hat{G}_i$. The reference states are generally non-orthogonal ($|s_{ij}| \in [0, 1]$), so in order to normalize $|\psi\rangle$ the coefficient vector \vec{c} is subject to the constraint that $\vec{c}^\dagger \mathbf{S} \vec{c} = 1$. The coefficients to minimize the expected energy are determined by solving the generalized eigenvalue problem

$$\mathbf{H}\mathbf{C} = \mathbf{S}\mathbf{C} \quad (25)$$

on a classical computer, such that the first column of \mathbf{C} corresponds to the lowest valued element E_1 of the diagonal eigenvalue matrix, \mathbf{E} , which approximates the low energy spectrum. Eq. 23 represents a natural extension of classical multi-reference methods which diagonalize within a basis of non-orthogonal Slater determinants [50], where the reference states are now chosen to be compact correlated wavefunctions. The matrix elements in Eqs. 24 can be efficiently resolved up to a constant additive error ϵ by a Hadamard test circuit [51], with $O(1/\epsilon^2)$ circuit repetitions for the overlap matrix elements and $O(\lambda^2/\epsilon^2)$ repetitions for the Hamiltonian matrix elements, where λ is the sum of absolute values of the coefficients in the JW decomposition of the Hamiltonian. There is generally no known classical algorithm to efficiently compute Eqs. 24 up to the corresponding levels of approximation, which is the basis for the claims of algorithmic quantum advantage in Refs. 7, 8.

Because the orbital rotations \hat{G}_{ij} are non-local operators, computing the *off-diagonal* ($i \neq j$) matrix elements can be highly non-trivial, even when the reference states $|\phi_i\rangle$ are independently classically simulable. Considering the combined state preparation circuit $\hat{U}_i |0\rangle = \hat{G}_i |\phi_i\rangle$, where $|0\rangle$ denotes the all-zero state, the diagonal matrix elements $h_{ii} = \langle \hat{U}_i^\dagger \hat{H} \hat{U}_i \rangle_0$ are expectation values of a local observable under unitary conjugation, which can be interpreted as dynamical evolution of \hat{H} in the Heisenberg picture, and may be exploitable by Pauli propagation methods [52]. The same argument cannot be applied to the off-diagonal matrix elements $h_{ij} = \langle \hat{U}_i^\dagger \hat{H} \hat{U}_j \rangle_0$, however,

which do not represent unitary conjugation. Preparing the multi-reference ansatz $(\sum_i c_i \hat{U}_i) |0\rangle$ on a single quantum register as a linear combination of unitaries (LCU) [53] would require a much deeper circuit, by at least a factor of M , composed of a highly structured sequence of controlled operations. By contrast, the quantum subspace framework allows for the variational flexibility of the ansatz to be increased systematically through the number of reference states, M , without increasing the circuit depth. These features of quantum multi-reference methods make them a promising avenue toward achieving practical quantum advantage in near-term chemical ground state preparation.

We now point out that Corollaries 1 and 2 apply to the rotated reference states for any choice of $|\phi_i\rangle$ that are sufficiently expressive to encode the product of fermionic magic states $|\Phi\rangle$ (as defined in Section IV). This places restrictions on any attempt at dequantization of the off-diagonal matrix element calculations in the hardest case. Corollary 1 immediately rules out any classical strategy which would provide an estimate of the matrix elements up to multiplicative precision. The Hadamard test circuit, however, computes an additive approximation of the matrix elements, so a successful dequantization need only match this level of accuracy. For sufficiently expressive reference states, prepared by generic quantum chemistry circuits of polynomial depth, an efficient classical approximation of Eqs. 24 up to additive precision is ruled out by Corollary 3 unless $\text{BQP} = \text{BPP}$.

It is harder to rule out the dequantization of Eqs. 24 up to an additive error for linear depth reference states prepared by restricted circuit families (see Sections VB and VC). However, certain attempts may be discounted, such as the mid-circuit ℓ^2 -norm sampling technique introduced in Ref. 27 (see Appendix D). Given efficient mid-circuit sampling and overlap query access in the computational basis, this algorithm could be used to efficiently compute $\langle \phi_i | \hat{G}_{ij} | \phi_j \rangle$ up to an additive error ϵ , using $O(1/\epsilon^2)$ samples. Supposing that the overlap $\langle \phi_i | x \rangle$ with a bitstring state $|x\rangle$ can be efficiently computed, Corollary 2 now rules out sampling $|x\rangle \sim \hat{G}_{ij} |\phi_j\rangle$. One could instead opt to sample from the distribution defined by $|\phi_j\rangle$, but it is then not possible to efficiently compute the overlaps $\langle \phi_i | \hat{G}_{ij} | x \rangle$, by Corollary 1. Note that it is not sufficient to estimate $\langle \phi_i | \hat{G}_{ij} | x \rangle$ up to an additive error (for example, by sampling $|y\rangle \sim |\phi_i\rangle$ and then efficiently computing $\langle y | \hat{G}_{ij} | x \rangle$ via Eq. 12), because an exponentially large number of samples would then be required to estimate $\langle \phi_i | \hat{G}_{ij} | \phi_j \rangle$ up to the same additive error (see Appendix D). Our worst case complexity results do not rule out the possibility of a decomposition $\hat{G}_{ij} = \hat{G}_a \hat{G}_b$ such that $\hat{G}_a^\dagger |\phi_i\rangle$ and $\hat{G}_b |\phi_j\rangle$ are simultaneously classically simulable, but there is no special structure in \hat{G}_{ij} suggestive of such a decomposition, so it is reasonable to assume that this will not be available in the hardest case.

B. TNQE (orbital-rotated MPS)

In the TNQE algorithm [8], the reference states in Eq. 23 are matrix product states,

$$|\phi_i\rangle = \sum_x \sum_{\{l\}}^{\chi} A_{l_p}^{x_p} A_{l_1}^{x_1} \cdots A_{l_{n-1}}^{x_{n-1}} |x\rangle, \quad (26)$$

where the $A_{l_{p-1}l_p}^{x_p}$ are three-index tensors with $2\chi^2$ elements corresponding to each fermionic mode, and χ is the bond dimension. It is implied in Eq. 26 that the tensor elements can be different for each reference state ($A = A^{(i)}$). The bond dimension bounds the Schmidt rank over any left-right bipartition of the sites, quantifying both the maximal entanglement of the quantum state and the classical memory requirement [54]. By setting χ to be independent of n , each MPS can be prepared by a quantum circuit of linear depth in n overall, with a constant depth on any one qubit [55–57]. In this low entanglement regime a single MPS can be efficiently contracted to compute the expectation value of an observable on a classical computer, and variationally optimized to minimize this value by the DMRG sweep algorithm [28, 58], thus efficiently representing the ground state of a gapped Hamiltonian satisfying a one-dimensional area law of entanglement [59]. This property, however, is not typical of chemical Hamiltonians describing Coulomb interactions in three-dimensional space (see Appendix F). The TNQE algorithm enables DMRG-like variational optimization of a quantum ansatz that does not follow the one-dimensional area law, since each reference state is expressed in molecular orbitals with a unique spatial distribution. Furthermore, in this quantum chemical setting, classical DMRG is considered to capture both static and dynamic correlations but to provide a much better treatment of the former [58, 60]. The quantum multi-reference TNQE enables a more flexible treatment of both types of electronic correlation, as can be seen by considering the Taylor expansion of Eq. 11, which is now shown to coincide with computational hardness.

Because any MPS can be chosen to be the tensor product of fermionic magic states $|\Phi\rangle$ with $\chi = 2$ (the magic state $|M\rangle$ as defined in Eq. 21 has a Schmidt rank of 2), our worst case simulation hardness results, Corollaries 1 and 2, must apply to the rotated reference states. To be clear, while it is possible to efficiently sample from any MPS $|\phi_i\rangle$ in its own *natural* single-particle basis, it is not in general classically efficient to sample from $\hat{G}_i |\phi_i\rangle$ as expressed in any *common* orbital basis. The overlap matrix element s_{ij} in Eqs. 24 is illustrated in Figure 4 in tensor network notation, where the orbital rotation \hat{G}_{ij} has been factorized into a linear depth sequence of Givens rotation gates. The Hamiltonian matrix elements h_{ij} can be computed by $O(n^4)$ tensor networks of this form, each of which has a Pauli string inserted between $|\phi_i\rangle$ and $\hat{G}_{ij} |\phi_j\rangle$ corresponding to a unique term in the JW decomposition of \hat{H}_i , which may be contracted into

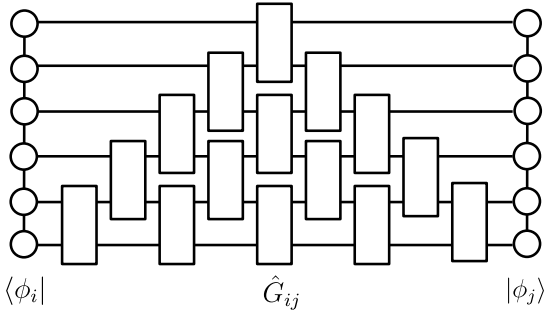


Figure 4. A tensor network to compute the overlap matrix element s_{ij} in Eqs. 24 between matrix product states $|\phi_i\rangle$ and $|\phi_j\rangle$ expressed in different orbital bases. The orbital rotation operator \hat{G}_{ij} has been factorized into a sequence of Givens rotation gates of depth $O(n)$ following Eq. 20. s_{ij} can be obtained up to an additive error ϵ by a linear depth Hadamard test circuit with $O(1/\epsilon^2)$ circuit repetitions [8]. The Hamiltonian matrix elements h_{ij} can be resolved up to error ϵ by $O(n^4)$ circuits of the same form with an inserted Pauli string, corresponding to the unique terms in the JW decomposition of \hat{H}_i , requiring $O(\lambda^2/\epsilon^2)$ circuit repetitions.

$|\phi_i\rangle$. Attempting to compute the value of the tensor network in Figure 4 by contracting each Givens rotation into either the MPS on the left or on the right results in a rapid explosion of the bond dimension. For Haar-random orbital rotations \hat{G} , the Slater determinant $\hat{G} |x\rangle$ exhibits a linearly scaling von Neumann entropy across any equal bipartition of the orbitals [61, 62], implying an exponentially large Schmidt rank (see e.g. Ref. 54). It follows that the truncation of $\hat{G}_{ij} |\phi_i\rangle$ to some fixed bond dimension $\chi = \text{poly}(n)$, for average case instances of \hat{G}_{ij} , will yield a vanishingly small fidelity in the limit of large n . This observed computational hardness is now formalized by Corollary 1, which states that the strong simulation of the hardest case matrix elements by classical tensor network contraction, or by some extension of the matchgate determinant calculation in Eq. 12, is GapP-hard. Furthermore, by Corollaries 1 and 2, dequantization up to an additive error by mid-circuit ℓ^2 -norm sampling is infeasible.

The classical intractability of TNQE in the hardest case is not surprising given prior results in tensor network theory. The cost of exact contraction for tensor networks designed to compactly represent ground states with an area law in two or more dimensions generally scales exponentially on classical computers [63]. Furthermore, approximate contraction of generic tensor networks of bounded degree, up to an additive error scale dependent on the tensor connectivity, is BQP-complete [32]. As an example, two-dimensional isometric PEPS (projected entangled pair states) can be directly mapped to a model of universal quantum computation [64], thus there is a computationally hard phase in which exact contraction is GapP-hard, and a constant additive approximation is BQP-complete. The separation in com-

plexity between approximating $\#P$ and GapP functions, which leads to exponential quantum speedups in sampling tasks [19, 24], has implications for approximate contraction schemes such as those based on quantum Monte Carlo (QMC) sampling [65]. In a related work it has been shown that positive bias in the tensor elements can render approximate tensor network contraction tractable [66]. However, fermionic systems present a unique challenge in this regard due to their antisymmetry under particle exchange, known in the context of QMC as the fermionic sign problem [67]. From this perspective, it is the combination of spatially local interactions in three dimensions, often lacking any translational symmetries, together with fermionic antisymmetry, which can make classical simulations of quantum chemistry so difficult. The TNQE algorithm is designed to address these challenging features of molecular systems with the minimal depth of quantum operations, which can be as low as $O(n)$ in the system size, as discussed above.

C. NOQE and UCCSD

The original NOQE ansatz [7] uses the same wavefunction form, that of Eq. 23, with UCCD reference states,

$$|\phi_i\rangle = \exp(\hat{T}_i - \hat{T}_i^\dagger) |x_0\rangle, \quad (27)$$

where the \hat{T}_i are two-body cluster operators of the form

$$\hat{T}_i = \sum_{pqrs} t_{pqrs}^{(i)} \hat{a}_p^\dagger \hat{a}_q^\dagger \hat{a}_r \hat{a}_s. \quad (28)$$

The orbital rotations \hat{G}_i in Eq. 23 transform between a set of M non-orthogonal unrestricted Hartree-Fock solutions (see Appendix F). Within each orbital basis the MOs are ordered by increasing energy, so the Hartree-Fock determinant $|x_0\rangle$ has the same expression in each basis. The parameters $t_{pqrs}^{(i)}$ are selected via classical methods, enabling the NOQE ansatz to capture both static and dynamic electron correlation, without hybrid variational optimization [7]. The orbital rotation operators \hat{G}_i represent one-body excitations via Eq. 11, so the rotated NOQE reference states $\hat{G}_i |\phi_i\rangle$ are equivalent to a partial Trotter decomposition of the unitary coupled-cluster ansatz with single and double excitations (UCCSD). It has been shown that PN non-conserving exponentiated single and double fermionic excitation generators constitute a universal gate set [45], as do non-fermionic and PN non-conserving generalizations of UCCSD [9]. For conserved PN, it has been shown that an infinite product of generalized unitary single and double excitation operators can parameterize any quantum state in the Fock space [68], but this has not previously been connected with computational hardness in the low depth regime. It is now implied by Theorem 2 that a generalized Trotter-decomposed UCCSD circuit can encode arbitrary logical computations with polynomial overhead

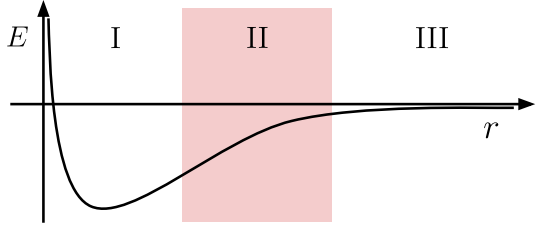


Figure 5. Schematic illustration of a molecular dissociation curve. The E -axis denotes energy and the r -axis denotes a molecular coordinate, e.g., a bond length. Region I corresponds to near-equilibrium ($r \approx r_0$) and Region III approaches the asymptotic limit of complete separation into two non-interacting fragments ($r \rightarrow \infty$). The intermediate Region II, the dissociation region, commonly exhibits a mixture of static and dynamic correlation effects, and CCSD or UCCSD descriptions of ground states in this regime commonly have large two-body cluster amplitudes ($|t_{pqrs}| \sim 1$) [71].

in the number of qubits and gates. Therefore, computing a constant additive approximation to the off-diagonal matrix elements is BQP -complete for polynomial depth reference states of this general form (Corollary 3).

For restricted variants of UCCSD designed to reduce the circuit depth, such as truncated low-rank factorizations of UCCD [69] or unitary cluster Jastrow (UCJ) [7, 70], the rotated NOQE reference states $\hat{G}_i |\phi_i\rangle$ remain sufficient for encoded universality under post-selection by Theorem 1 (see Appendix E). For the UCCD state in Eq. 27, the tensor product of magic states $|\Phi\rangle$ (defined in Section IV) is preparable using a two-body cluster operator with amplitudes $t_{pqrs} \in \{0, \pm \frac{\pi}{4}\}$ and subsequent Givens rotations (see Appendix E). Corollaries 1 and 2 then apply to $\hat{G}_i |\phi_i\rangle$, namely GapP -hardness of strong simulation (Corollary 1) and classical hardness of random sampling (Corollary 2), under the assumption that the polynomial hierarchy is infinite. In practice, computational hardness is observed in the Taylor expansion of the cluster exponential to classically approximate the off-diagonal matrix elements. While truncation to finite order enables contributions from $\text{poly}(n)$ excited determinants, the anticoncentration theorem of Oszmaniec *et al.* [22] (Theorem 4) implies that for Haar-random \hat{G}_i there is likely to be non-negligible support on exponentially many determinants. Recall that classically approximating the output probabilities of a quantum register, or sampling from its distribution, can be harder than classically estimating the expectation value of a local observable, which represents unitary conjugation under the state preparation circuit. The off-diagonal matrix elements in quantum multi-reference methods, however, do not represent unitary conjugation, and in general computing them is as hard as closed simulation.

Molecular systems are typically well described by single-reference coupled-cluster theories around their equilibrium geometry (Region I in Figure 5). In this perturbative (dynamic correlation) regime the ground

state wavefunction is dominated by a single Hartree-Fock Slater determinant, and the two-body amplitudes are small ($|t_{pqrs}| \ll 1$) [72]. The wavefunction is then well approximated by a truncated Taylor expansion of the projective CCSD ansatz, the closest tractable classical analogue of the UCCSD ansatz [10], and empirical studies do not suggest a quantum advantage for such systems [60, 73]. While molecules most commonly occupy their equilibrium configurations under ambient conditions, the *dissociation region* (Region II in Figure 5) is vital for understanding chemical phenomena related to bond breaking and formation, reaction kinetics, and catalysis. Empirically this regime often incurs large \hat{T} amplitudes ($|t_{pqrs}| \sim 1$), and the projective coupled-cluster approximation breaks down [71, 72]. Although there is no single accepted definition of static electron correlation — a term which connotes the strongly multi-reference character of the wavefunction [46–48] (see Appendix F) — large amplitudes in \hat{T} are considered an indicator [47, 71], so this regime is characterized by a mixture of static and dynamic correlation effects. The results in this work show that, for particular instances of UCCSD where $|t_{pqrs}| \in \{0, \frac{\pi}{4}\}$, classical simulation is not possible by any efficient heuristic unless the polynomial hierarchy collapses. Two-body amplitudes t_{pqrs} of magnitude $\sim \frac{\pi}{4}$ are quite common for correlated electronic states within this regime [71], supporting the view that systems exhibiting both static and dynamic electron correlation are prime candidates for achieving exponential quantum advantage in quantum chemistry.

VI. CONCLUSION

We have shown that orbital rotation circuits with fermionic magic state inputs are not classically simulable in the worst case, in either the strong or weak sense, under the assumption that the polynomial hier-

archy is infinite. We then applied this result to multi-reference hybrid quantum-classical methods for chemical ground state preparation — namely TNQE [8] and NOQE [7] — which provide an algorithmic quantum advantage (there is no known tractable classical analogue for systems exhibiting both static and dynamic electron correlation that is both variational and size-consistent). This suggests that chemical ground states for large complex systems that are characterized by both types of correlation will require a quantum computer to be efficiently computed using a scalable wavefunction ansatz. The main result of this paper (Theorem 1) now rules out in the worst case any classical simulation algorithm that would require, or otherwise enable, efficient closed simulation of the output probabilities of these quantum ansätze up to a multiplicative factor, or efficient sampling from their probability distributions, under the generalized $P \neq NP$ conjecture. We present this as evidence that super-polynomial quantum speedups in quantum chemistry are theoretically achievable on near-term hardware, using circuits of linear depth in the system size. We conclude that useful speedups are most likely to be found for systems possessing both static and dynamic electron correlations, exemplified by molecular systems undergoing bond breaking and catalysis, and systems possessing multiple unpaired electrons or multivalent metal atoms.

VII. ACKNOWLEDGEMENTS

We thank Jiaqing Jiang, Dominik Hangleiter, and Zeph Landau for helpful discussions. This work was supported by the NSF QLCI program through grant number QMA-2016345, partially by the U.S. Department of Energy, Office of Science, Office of Advanced Scientific Computing Research under Award Number DE-SC0025526, and as part of a joint development agreement between UC Berkeley and Dow.

[1] D. Shepherd and M. J. Bremner, *Proceedings of the Royal Society A: Mathematical, Physical and Engineering Sciences* **465**, 1413 (2009), publisher: Royal Society.

[2] M. J. Bremner, R. Jozsa, and D. J. Shepherd, *Proceedings of the Royal Society A: Mathematical, Physical and Engineering Sciences* **467**, 459 (2010), publisher: Royal Society.

[3] S. Aaronson and L. Chen, in *Proceedings of the 32nd Computational Complexity Conference, CCC '17* (Schloss Dagstuhl-Leibniz-Zentrum fuer Informatik, Dagstuhl, DEU, 2017) pp. 1–67.

[4] F. Arute, K. Arya, R. Babbush, D. Bacon, J. C. Bardin, R. Barends, R. Biswas, S. Boixo, F. G. S. L. Brandao, D. A. Buell, B. Burkett, Y. Chen, Z. Chen, B. Chiaro, R. Collins, W. Courtney, A. Dunsworth, E. Farhi, B. Foxen, A. Fowler, C. Gidney, M. Giustina, R. Graff, K. Guerin, S. Habegger, M. P. Harrigan, M. J. Hartmann, A. Ho, M. Hoffmann, T. Huang, T. S. Humble, S. V. Isakov, E. Jeffrey, Z. Jiang, D. Kafri, K. Kechedzhi, J. Kelly, P. V. Klimov, S. Knyshev, A. Korotkov, F. Kostritsa, D. Landhuis, M. Lindmark, E. Lucero, D. Lyakh, S. Mandrà, J. R. McClean, M. McEwen, A. Megrant, X. Mi, K. Michelsen, M. Mohseni, J. Mutus, O. Naaman, M. Neeley, C. Neill, M. Y. Niu, E. Ostby, A. Petukhov, J. C. Platt, C. Quintana, E. G. Rieffel, P. Roushan, N. C. Rubin, D. Sank, K. J. Satzinger, V. Smelyanskiy, K. J. Sung, M. D. Tervitthick, A. Vainsencher, B. Villalonga, T. White, Z. J. Yao, P. Yeh, A. Zalcman, H. Neven, and J. M. Martinis, *Nature* **574**, 505 (2019), publisher: Nature Publishing Group.

[5] S. Ghosh, A. Deshpande, D. Hangleiter, A. V. Gorshkov, and B. Fefferman, *Physical Review Letters* **131**, 030601 (2023), publisher: American Physical Society.

[6] A. Peruzzo, J. McClean, P. Shadbolt, M.-H. Yung, X.-Q. Zhou, P. J. Love, A. Aspuru-Guzik, and J. L. O’Brien,

Nature Communications **5**, 4213 (2014), publisher: Nature Publishing Group.

[7] U. Baek, D. Hait, J. Shee, O. Leimkuhler, W. J. Huggins, T. F. Stetina, M. Head-Gordon, and K. B. Whaley, **PRX Quantum** **4**, 030307 (2023), publisher: American Physical Society.

[8] O. Leimkuhler and K. B. Whaley, “A quantum eigenvalue solver based on tensor networks,” (2024), arXiv:2404.10223 [quant-ph].

[9] J. R. McClean, J. Romero, R. Babbush, and A. Aspuru-Guzik, **New Journal of Physics** **18**, 023023 (2016), publisher: IOP Publishing.

[10] A. Anand, P. Schleich, S. Alperin-Lea, P. W. K. Jensen, S. Sim, M. Díaz-Tinoco, J. S. Kottmann, M. Degroote, A. F. Izmaylov, and A. Aspuru-Guzik, **Chemical Society Reviews** **51**, 1659 (2022), publisher: The Royal Society of Chemistry.

[11] J. Tilly, H. Chen, S. Cao, D. Picozzi, K. Setia, Y. Li, E. Grant, L. Wossnig, I. Rungger, G. H. Booth, and J. Tennyson, **Physics Reports The Variational Quantum Eigensolver: a review of methods and best practices**, **986**, 1 (2022).

[12] L. G. Valiant, **SIAM Journal on Computing** **31**, 1229 (2002), publisher: Society for Industrial and Applied Mathematics.

[13] B. M. Terhal and D. P. DiVincenzo, **Physical Review A** **65**, 032325 (2002), publisher: American Physical Society.

[14] R. Jozsa and A. Miyake, **Proceedings of the Royal Society A: Mathematical, Physical and Engineering Sciences** **464**, 3089 (2008), publisher: Royal Society.

[15] I. D. Kivlichan, J. McClean, N. Wiebe, C. Gidney, A. Aspuru-Guzik, G. K.-L. Chan, and R. Babbush, **Physical Review Letters** **120**, 110501 (2018), publisher: American Physical Society.

[16] Z. Jiang, K. J. Sung, K. Kechedzhi, V. N. Smelyanskiy, and S. Boixo, **Physical Review Applied** **9**, 044036 (2018), publisher: American Physical Society.

[17] M. Hebenstreit, R. Jozsa, B. Kraus, S. Strelchuk, and M. Yoganathan, **Physical Review Letters** **123**, 080503 (2019), publisher: American Physical Society.

[18] M. Hebenstreit, R. Jozsa, B. Kraus, and S. Strelchuk, **Physical Review A** **102**, 052604 (2020), publisher: American Physical Society.

[19] D. Hangleiter and J. Eisert, **Reviews of Modern Physics** **95**, 035001 (2023), publisher: American Physical Society.

[20] K. Fujii and T. Morimae, **New Journal of Physics** **19**, 033003 (2017), publisher: IOP Publishing.

[21] D. A. Ivanov, **Physical Review A** **96**, 012322 (2017), publisher: American Physical Society.

[22] M. Oszmaniec, N. Dangniam, M. E. Morales, and Z. Zimborás, **PRX Quantum** **3**, 020328 (2022), publisher: American Physical Society.

[23] L. Stockmeyer, in *Proceedings of the fifteenth annual ACM symposium on Theory of computing - STOC '83* (ACM Press, Not Known, 1983) pp. 118–126.

[24] S. Aaronson and A. Arkhipov, in *Proceedings of the forty-third annual ACM symposium on Theory of computing*, STOC '11 (Association for Computing Machinery, New York, NY, USA, 2011) pp. 333–342.

[25] W. J. Huggins, J. Lee, U. Baek, B. O'Gorman, and K. B. Whaley, **New Journal of Physics** **22**, 073009 (2020), publisher: IOP Publishing.

[26] D. Marti-Dafcik, H. G. A. Burton, and D. P. Tew, **Physical Review Research** **7**, 013191 (2025), publisher: American Physical Society.

[27] E. Tang, in *Proceedings of the 51st Annual ACM SIGACT Symposium on Theory of Computing*, STOC 2019 (Association for Computing Machinery, New York, NY, USA, 2019) pp. 217–228.

[28] S. R. White, **Physical Review Letters** **69**, 2863 (1992), publisher: American Physical Society.

[29] S. Toda, **SIAM Journal on Computing** **20**, 865 (1991), publisher: Society for Industrial and Applied Mathematics.

[30] C. Lautemann, **Information Processing Letters** **17**, 215 (1983).

[31] M. A. Nielsen and I. L. Chuang, “Quantum Computation and Quantum Information: 10th Anniversary Edition,” (2010), ISBN: 9780511976667 Publisher: Cambridge University Press.

[32] I. Arad and Z. Landau, **SIAM Journal on Computing** **39**, 3089 (2010).

[33] S. Aaronson, **Proceedings of the Royal Society A: Mathematical, Physical and Engineering Sciences** **461**, 3473 (2005), publisher: Royal Society.

[34] Y. Han, L. A. Hemaspaandra, and T. Thierauf, **SIAM Journal on Computing** **26**, 59 (1997).

[35] T. Helgaker, P. Jørgensen, and J. Olsen, in *Molecular Electronic-Structure Theory* (John Wiley & Sons, Ltd, 2000) pp. 1–33.

[36] J. Surace and L. Tagliacozzo, **SciPost Physics Lecture Notes** , 054 (2022).

[37] D. J. Thouless, **Nuclear Physics** **21**, 225 (1960).

[38] P. Jordan and E. Wigner, **Zeitschrift für Physik** **47**, 631 (1928).

[39] E. Knill, “Fermionic Linear Optics and Matchgates,” (2001), arXiv:quant-ph/0108033.

[40] F. Verstraete, J. I. Cirac, and J. I. Latorre, **Physical Review A** **79**, 032316 (2009), publisher: American Physical Society.

[41] I. L. Chuang and Y. Yamamoto, **Physical Review A** **52**, 3489 (1995), publisher: American Physical Society.

[42] J. M. Arrazola, O. D. Matteo, N. Quesada, S. Jahangiri, A. Delgado, and N. Killoran, **Quantum** **6**, 742 (2022), publisher: Verein zur Förderung des Open Access Publizierens in den Quantenwissenschaften.

[43] M. Oszmaniec and Z. Zimborás, **Physical Review Letters** **119**, 220502 (2017), publisher: American Physical Society.

[44] G. Vidal and C. M. Dawson, **Physical Review A** **69**, 010301 (2004), publisher: American Physical Society.

[45] S. B. Bravyi and A. Y. Kitaev, **Annals of Physics** **298**, 210 (2002).

[46] D. P. Tew, W. Klopper, and T. Helgaker, **Journal of Computational Chemistry** **28**, 1307 (2007).

[47] B. Ganoe and J. Shee, **Faraday Discussions** **254**, 53 (2024), publisher: The Royal Society of Chemistry.

[48] R. Izsák, A. V. Ivanov, N. S. Blunt, N. Holzmann, and F. Neese, **Journal of Chemical Theory and Computation** **19**, 2703 (2023), publisher: American Chemical Society.

[49] M. Motta, W. Kirby, I. Liepuoniate, K. J. Sung, J. Cohn, A. Mezzacapo, K. Klymko, N. Nguyen, N. Yoshioka, and J. E. Rice, **Electronic Structure** **6**, 013001 (2024), publisher: IOP Publishing.

[50] A. J. W. Thom and M. Head-Gordon, **The Journal of Chemical Physics** **131**, 124113 (2009).

[51] R. Cleve, A. Ekert, C. Macchiavello, and M. Mosca, **Proceedings of the Royal Society of London. Series A: Mathematical, Physical and Engineering Sciences** **454**, 1239 (1998).

Mathematical, Physical and Engineering Sciences **454**, 339 (1998), publisher: Royal Society.

[52] A. Angrisani, A. Schmidhuber, M. S. Rudolph, M. Cerezo, Z. Holmes, and H.-Y. Huang, “Classically estimating observables of noiseless quantum circuits,” (2024), arXiv:2409.01706 [quant-ph].

[53] A. M. Childs and N. Wiebe, Quantum Info. Comput. **12**, 901 (2012).

[54] G. Vidal, Physical Review Letters **91**, 147902 (2003), publisher: American Physical Society.

[55] C. Schön, E. Solano, F. Verstraete, J. I. Cirac, and M. M. Wolf, Physical Review Letters **95**, 110503 (2005), publisher: American Physical Society.

[56] S.-J. Ran, Physical Review A **101**, 032310 (2020), publisher: American Physical Society.

[57] S. Fomichev, K. Hejazi, M. S. Zini, M. Kiser, J. Fraxanet, P. A. M. Casares, A. Delgado, J. Huh, A.-C. Voigt, J. E. Mueller, and J. M. Arrazola, PRX Quantum **5**, 040339 (2024), publisher: American Physical Society.

[58] A. Baiardi and M. Reiher, The Journal of Chemical Physics **152**, 040903 (2020).

[59] M. B. Hastings, Journal of Statistical Mechanics: Theory and Experiment **2007**, P08024 (2007).

[60] G. K.-L. Chan, Faraday Discussions **254**, 11 (2024), publisher: The Royal Society of Chemistry.

[61] P. Lydżba, M. Rigol, and L. Vidmar, Physical Review Letters **125**, 180604 (2020), publisher: American Physical Society.

[62] E. Bianchi, L. Hackl, and M. Kieburg, Physical Review B **103**, L241118 (2021), publisher: American Physical Society.

[63] N. Schuch, M. M. Wolf, F. Verstraete, and J. I. Cirac, Physical Review Letters **98**, 140506 (2007), publisher: American Physical Society.

[64] D. Malz and R. Trivedi, “Computational complexity of isometric tensor network states,” (2024), arXiv:2402.07975 [quant-ph].

[65] N. Schuch, M. M. Wolf, F. Verstraete, and J. I. Cirac, Physical Review Letters **100**, 040501 (2008), publisher: American Physical Society.

[66] J. Chen, J. Jiang, D. Hangleiter, and N. Schuch, PRX Quantum **6**, 010312 (2025), publisher: American Physical Society.

[67] M. Troyer and U.-J. Wiese, Physical Review Letters **94**, 170201 (2005), publisher: American Physical Society.

[68] F. A. Evangelista, G. K.-L. Chan, and G. E. Scuseria, The Journal of Chemical Physics **151**, 244112 (2019).

[69] M. Motta, E. Ye, J. R. McClean, Z. Li, A. J. Minnich, R. Babbush, and G. K.-L. Chan, npj Quantum Information **7**, 1 (2021), publisher: Nature Publishing Group.

[70] Y. Matsuzawa and Y. Kurashige, Journal of Chemical Theory and Computation **16**, 944 (2020), publisher: American Chemical Society.

[71] I. M. B. Nielsen and C. L. Janssen, Chemical Physics Letters **310**, 568 (1999).

[72] T. Helgaker, P. Jørgensen, and J. Olsen, in *Molecular Electronic-Structure Theory* (John Wiley & Sons, Ltd, 2000) pp. 648–723.

[73] S. Lee, J. Lee, H. Zhai, Y. Tong, A. M. Dalzell, A. Kumar, P. Helms, J. Gray, Z.-H. Cui, W. Liu, M. Kastoryano, R. Babbush, J. Preskill, D. R. Reichman, E. T. Campbell, E. F. Valeev, L. Lin, and G. K.-L. Chan, Nature Communications **14**, 1952 (2023), publisher: Nature Publishing Group.

[74] D. Aharonov, “A Simple Proof that Toffoli and Hadamard are Quantum Universal,” (2003), arXiv:quant-ph/0301040.

Appendix A: Dual-rail encodings for one- and two-qubit gates

A logical single qubit rotation can be decomposed into a sequence of Euler angle rotations [31] as

$$U = R_z(\varphi_1)R_y(\theta)R_z(\varphi_2), \quad (\text{A1})$$

up to a global phase, where

$$R_z(\varphi) = \begin{pmatrix} e^{-i\frac{\varphi}{2}} & 0 \\ 0 & e^{i\frac{\varphi}{2}} \end{pmatrix}, \quad (\text{A2})$$

$$R_y(\theta) = \begin{pmatrix} \cos(\frac{\theta}{2}) & -\sin(\frac{\theta}{2}) \\ \sin(\frac{\theta}{2}) & \cos(\frac{\theta}{2}) \end{pmatrix}. \quad (\text{A3})$$

Under the dual-rail encoding, the $|0\rangle$, $|1\rangle$ states are mapped to the $|01\rangle$, $|10\rangle$ states respectively (the $|00\rangle$ and $|11\rangle$ states of the dual-rail are not accessed throughout the computation). Now the PN conserving matchgates

$$R(\varphi) \otimes \mathbb{1} = \begin{pmatrix} 1 & 0 & 0 & 0 \\ 0 & 1 & 0 & 0 \\ 0 & 0 & e^{i\varphi} & 0 \\ 0 & 0 & 0 & e^{i\varphi} \end{pmatrix}, \quad (\text{A4})$$

$$G(\theta/2) = \begin{pmatrix} 1 & 0 & 0 & 0 \\ 0 & \cos(\frac{\theta}{2}) & -\sin(\frac{\theta}{2}) & 0 \\ 0 & \sin(\frac{\theta}{2}) & \cos(\frac{\theta}{2}) & 0 \\ 0 & 0 & 0 & 1 \end{pmatrix}, \quad (\text{A5})$$

where $G(\theta/2)$ is a Givens rotation by $\theta/2$ in the single excitation subspace, encode the exact same computations as the logical single-qubit R_z and R_y gates within the single-particle block, up to an unimportant global phase. Hence the circuit decomposition in Figure 1 implements an arbitrary logical single-qubit rotation in the dual-rail encoding.

In the logical space, an arbitrary two-qubit unitary decomposes into three CNOT gates interleaved with single-qubit rotations [44]. A CNOT gate can be further decomposed into a CZ gate conjugated by Hadamard gates on the target qubit. Hence the same two-qubit gate decomposition can be achieved with three CZ gates interleaved with single-qubit rotations. In the dual-rail encoding, a logical CZ operation induces a phase flip on the $|1010\rangle$ basis vector, leaving the other dual-rail computational basis vectors ($|1001\rangle$, $|0110\rangle$, $|0101\rangle$) unchanged. This can be achieved using only nearest-neighbor gates by a CZ gate acting on the middle two qubits followed by a Z gate on the third qubit, inducing a resultant phase flip only when the middle two qubits are in the $|01\rangle$ state. Then by decomposing each logical single-qubit rotation into Euler angles and encoding within the dual-rail space according to Figure 1, followed by some rearrangement

of the phase gates, we arrive at the dual-rail circuit decomposition of an arbitrary logical two-qubit gate shown in Figure 2.

Note that the CZ gate acting between neighboring dual-rail qubits generates entanglement through a controlled phase flip, thus requiring no transport of particles between the dual-rails. The transmission of logical quantum information is thus entirely by means of entangling the phases of the dual-rail qubit states. Note also that encoded universality, and the implementation of arbitrary logical two-qubit gates, is only possible because the CZ gate is not a matchgate. Attempting to draw an equivalence between the CZ gate,

$$CZ = \begin{pmatrix} 1 & 0 & 0 & 0 \\ 0 & 1 & 0 & 0 \\ 0 & 0 & 1 & 0 \\ 0 & 0 & 0 & -1 \end{pmatrix}, \quad (A6)$$

and the matchgate definition (Eq. 14), we would have that

$$\mathbf{u} = \begin{pmatrix} 1 & 0 \\ 0 & -1 \end{pmatrix}, \quad \mathbf{v} = \begin{pmatrix} 1 & 0 \\ 0 & 1 \end{pmatrix}, \quad (A7)$$

so that $\det(\mathbf{u}) = -\det(\mathbf{v})$. It is worth remarking that this single phase difference between the submatrix determinants is sufficient to elevate the classically simulable family of PN conserving matchgate circuits to a universal model of quantum computation.

In Ref. 42 it was shown that the controlled single excitation gate is a universal gate for quantum chemistry circuits, meaning that any wavefunction in the PN conserving subspace may be constructed using only this gate. In our scheme, a logical controlled- U gate maps directly to a controlled single excitation gate in the dual-rail encoding. Since any logical two-qubit gate may be implemented as in Fig. 2, it follows that the controlled single excitation gate is equivalent to a construction of Givens and phase rotations and CZ gates. This construction can be explicitly derived starting from the decomposition of the controlled- U gate into two CNOT gates and three single-qubit rotations on the target qubit (see Figure 4.6 in Ref. 31). By expanding the target qubit into a dual-rail representation, the logical single qubit rotations are replaced by single excitation gates on the dual-rail qubit, and the CNOT gates are replaced by CSWAP gates which may be further decomposed into controlled-Z gates and additional single excitation gates on the dual-rail qubit. Each single excitation gate may then be factorized into a product of phase and Givens rotation gates following the decomposition of the logical single-qubit rotation of the $|10\rangle$ and $|01\rangle$ states of the dual-rail qubit into Euler rotations. To complete the construction, the logical rotation $R_z(\varphi)$ may be implemented in the dual-rail representation without incurring a spurious phase on the $|11\rangle$ state of the dual-rail qubit by the product of $R(\varphi/2) \otimes R^\dagger(\varphi/2)$. Therefore, nearest-neighbor Givens and phase rotations plus CZ gates are a universal gate set for quantum chemistry, which may be of utility in the design of universal PN

conserving ‘brick-wall’ circuits for architectures in which the CZ gate is cheaper to implement than the generic SWAP gate.

Appendix B: Implementing the CZ gate under post-selection

The CZ gate between two qubits in computational basis state $|xy\rangle$, where $x, y \in \{0, 1\}$, maps

$$|xy\rangle \mapsto (-1)^{x \cdot y} |xy\rangle. \quad (B1)$$

This operation cannot be implemented with matchgates alone, but can be implemented under post-selection with access to a four qubit, two particle magic state

$$|M'\rangle = \frac{1}{2} (|1001\rangle + |1010\rangle + |0101\rangle - |0110\rangle), \quad (B2)$$

where we have used $|M'\rangle$ to distinguish this from the magic state in Eq. 21. By post-selection we mean that the outcome of a measurement can be enforced, equivalent to projecting onto the desired measurement outcome and re-normalizing the projected quantum state. Consider the projectors $|\tilde{\pm}\rangle \langle \tilde{\pm}|$ which project onto the two-qubit Bell states

$$|\tilde{\pm}\rangle \equiv \frac{1}{\sqrt{2}} (|01\rangle \pm |10\rangle). \quad (B3)$$

Then it can be shown that

$$(|\tilde{+}\rangle \langle \tilde{+}| \otimes \mathbf{1} \otimes |\tilde{+}\rangle \langle \tilde{+}|) |x\rangle |M'\rangle |y\rangle \quad (B4)$$

$$= \frac{(-1)^{x \cdot y}}{2} |\tilde{+}\rangle |xy\rangle |\tilde{+}|. \quad (B5)$$

The projection onto the $|\tilde{+}\rangle$ state can be achieved by rotating into the $|\tilde{+}\rangle, |\tilde{-}\rangle$ basis via a Givens rotation with angle $\theta = \pi/4$ and measuring the $|10\rangle$ state.

To implement a logical quantum circuit with multiple layers of two-qubit gates under post-selection, we require a protocol to swap the magic state in-between the target qubits as needed and then to swap the measurement qubits out to the end of the circuit so that successive logical operations can be applied. This can be achieved using fermionic SWAP (FSWAP) gates, which are particle-number conserving matchgates. When two registers are interchanged via an FSWAP network, a -1 phase is incurred whenever the ordering of two particles is interchanged. Since the magic state $|M'\rangle$ has an even number of particles it can be freely moved to any position in the circuit via an FSWAP network without incurring any resultant phase flips. After the application of the Givens rotations, and prior to measurement, rearranging the top and middle qubit pairs incurs an additional phase flip whenever the top qubits are in the $|\tilde{+}\rangle$ state and the middle qubits are in the states $|xy\rangle = |10\rangle$ or $|01\rangle$. These phase flips can be incorporated into the magic state which yields Eq. 21. Putting these steps together results in

the gadget in Figure 3 to implement the CZ gate under post-selection, where the bottom four-qubit register can be freely moved around the circuit using FSWAP gates both before and after applying the gadget (and prior to measurement).

Appendix C: Universality under post-selection with real-valued orbital rotations

Under the Jordan-Wigner mapping, the single-qubit phase gate $R(\varphi)$ is equivalent to a complex phase change on one of the orbitals (see Eq. 17). We now show that universal quantum computation can be achieved under post-selection using only real-valued PN-conserving matchgates. This follows from the well known fact that a complex-valued unitary computation can be encoded within a real-valued one by the use of ancilla qubits (see e.g. Ref. 74). For example, consider a single qubit in the state

$$(a + ib)|0\rangle + (c + id)|1\rangle, \quad (\text{C1})$$

where

$$|a + ib|^2 + |c + id|^2 = |a|^2 + |b|^2 + |c|^2 + |d|^2 = 1. \quad (\text{C2})$$

We may equivalently encode this quantum state with an additional ancilla qubit that represents the complex phase as

$$a|00\rangle + b|01\rangle + c|10\rangle + d|11\rangle. \quad (\text{C3})$$

Now consider the implementation of the complex phase gate $R(\varphi)$ which shifts the phase of the $|1\rangle$ state by $e^{i\varphi} = \cos\varphi + i\sin\varphi$. The same transformation of the coefficients can be achieved in the real-valued encoding by a controlled- R_y gate on the second qubit with control from the first qubit. By adding a separate phase qubit for each system qubit, it is then straightforward to see that an arbitrary quantum circuit can be implemented within this encoding using only orthogonal nearest-neighbor two-qubit gates (including SWAP gates). Then this logical real-valued circuit may be encoded under post-selection within the PN conserving dual-rail representation with entirely real-valued matchgates and magic state inputs, where each logical qubit is now represented by four physical qubits instead of two.

Appendix D: Additive error dequantization by mid-circuit ℓ^2 -norm sampling

Here we summarize a dequantization scheme for overlap matrix elements of the form $\langle y|\hat{U}|x\rangle$ based on mid-circuit ℓ^2 -norm sampling, adapted from the overlap estimation technique introduced in Ref. 27. We then show that access to an additive error approximation for the mid-circuit overlaps is insufficient to obtain an additive error approximation for $\langle y|\hat{U}|x\rangle$.

First, let $\hat{U} = \hat{U}_a \hat{U}_b$, such that $|\phi\rangle = \hat{U}_b|x\rangle$ and $|\psi\rangle = \hat{U}_a^\dagger|y\rangle$ are real-valued normalized wavefunctions, so that $\langle y|\hat{U}|x\rangle = \langle\psi|\phi\rangle$. Let this decomposition be chosen such that $|\psi\rangle, |\phi\rangle$ are both strongly simulable, i.e., the overlaps $\phi_z = \langle z|\phi\rangle$ and $\psi_z = \langle z|\psi\rangle$ are efficiently computable for any computational basis vector $|z\rangle$. Furthermore, let $|\phi\rangle$ be weakly simulable, i.e., we may efficiently sample $|z\rangle \sim P(z) = \phi_z^2$. Now let \mathcal{Z} be the random variable ψ_z/ϕ_z , which is efficiently computable for any $|z\rangle$, sampled with probability $P(z) = \phi_z^2$. Then

$$\mathbb{E}[\mathcal{Z}] = \sum_z P(z) \frac{\psi_z}{\phi_z} = \sum_z \psi_z \phi_z = \langle\psi|\phi\rangle, \quad (\text{D1})$$

$$\text{Var}[\mathcal{Z}] \leq \sum_z P(z) \left(\frac{\psi_z}{\phi_z} \right)^2 = \sum_z \psi_z^2 = 1. \quad (\text{D2})$$

Because $\text{Var}[\mathcal{Z}]$ is bounded by a constant, we may efficiently compute an additive error approximation to $\langle\psi|\phi\rangle$ with $O(1/\epsilon^2)$ samples, completely independent of the number of qubits n .

However, suppose now that $\psi_z = \langle z|\psi\rangle$ is not strongly simulable, but can itself be computed up to an additive error. For example, suppose that when ψ_z is queried by some randomized classical algorithm, one instead obtains $\psi_z + \mathcal{E}$ in computation time t , where \mathcal{E} is a random variable with mean zero and variance $\sigma^2 \propto 1/t$. Let \mathcal{Z}' be the random variable $(\psi_z + \mathcal{E})/\phi_z$ thus obtained when $|z\rangle$ is sampled from $P(z) = \phi_z^2$. Let us choose $|\phi\rangle$ to be the tensor product of magic states, $|M\rangle^{\otimes m}$, where for simplicity $|M\rangle = \frac{1}{\sqrt{2}}(|1100\rangle + |0011\rangle)$, which is related to Eq. 21 by a matchgate circuit. Then $|\phi\rangle$ has uniform support over 2^m computational basis vectors seen by expanding the tensor product (let us denote this set of computational basis vectors by \mathcal{M}), i.e.,

$$\phi_z = \begin{cases} 2^{-\frac{m}{2}} & |z\rangle \in \mathcal{M}, \\ 0 & |z\rangle \notin \mathcal{M}. \end{cases} \quad (\text{D3})$$

Considering only $|z\rangle \in \mathcal{M}$, which may be obtained by sampling from $|\phi\rangle$, then we may write $\mathcal{Z}' = \mathcal{Z} + 2^{\frac{m}{2}}\mathcal{E}$, which is the sum of two independent random variables (the distribution of \mathcal{E} is assumed not to depend on the value of ψ_z). We then have that

$$\mathbb{E}[\mathcal{Z}'] = \mathbb{E}[\mathcal{Z}] + \mathbb{E}[2^{\frac{m}{2}}\mathcal{E}] = \langle\psi|\phi\rangle, \quad (\text{D4})$$

$$\text{Var}[\mathcal{Z}'] = \text{Var}[\mathcal{Z}] + \text{Var}[2^{\frac{m}{2}}\mathcal{E}] \geq 2^m\sigma^2. \quad (\text{D5})$$

Although the mean value is correct, the variance of \mathcal{Z}' now scales exponentially with the number of magic states m , and thus with the total number of qubits n , so the number of samples that would be required to evaluate $\langle\psi|\phi\rangle$ up to an additive error will also scale exponentially in the system size. Or, put another way, suppressing the variance in the partial overlaps to some constant independent of n would require a computation time $t \propto 2^{\frac{n}{4}}$.

Appendix E: Fermionic magic state preparation via two-body excitations and construction of $\hat{G}|\Phi\rangle$

Here we show how to prepare the state $|\Phi\rangle = |01\rangle^{\otimes\nu} \otimes |M\rangle^{\otimes 3\mu}$ of Theorem 1 in the main text, with $|M\rangle$ a four-qubit fermionic magic state (defined in Eq. 21), starting from a Hartree-Fock determinant $|x_0\rangle$ and applying two-body excitation terms and subsequent Givens rotations. From this it follows that the rotated NOQE reference states can encode any instance of $\hat{G}|\Phi\rangle$. We then extend this to arbitrary Trotter decompositions of the UCCSD ansatz. First, let $\eta = n/2 = \nu + 6\mu$. The initial determinant $|x_0\rangle$ then has η zeros followed by η ones. There exists an FSWAP network \hat{F} which rearranges the elements such that

$$\hat{F}|x_0\rangle = |01\rangle^{\otimes\nu} \otimes |1001\rangle^{\otimes 3\mu}. \quad (\text{E1})$$

Now we define the four-qubit double-excitation gate,

$$\tau_p(\theta) = \exp(\theta(\hat{a}_{p+1}^\dagger \hat{a}_{p+2}^\dagger \hat{a}_{p+3} \hat{a}_p - \text{h.c.})). \quad (\text{E2})$$

Then on a four-qubit register with $p = 1, \dots, 4$ we have

$$\tau_1(\pi/4)|1001\rangle = \frac{1}{\sqrt{2}}(|1001\rangle + |0110\rangle). \quad (\text{E3})$$

Applying a $\theta = \pi/4$ Givens rotation between the last two qubits and a $\theta = \pi$ Givens rotation between the middle two qubits prepares the desired fermionic magic state,

$$|M\rangle = G_2(\pi)G_3(\pi/4)\tau_1(\pi/4)|1001\rangle. \quad (\text{E4})$$

Then we may write

$$|\Phi\rangle = \hat{G} \exp(\hat{T} - \hat{T}^\dagger) \hat{F} |x_0\rangle, \quad (\text{E5})$$

with

$$\hat{G} = \prod_{k=1}^{3\mu} G_{q(k)+2}(\pi/4)G_{q(k)+3}(\pi), \quad (\text{E6})$$

$$\exp(\hat{T} - \hat{T}^\dagger) = \prod_{k=1}^{3\mu} \tau_{q(k)+1}(\pi/4), \quad (\text{E7})$$

where $q(k) = 2n + 4(k-1)$, and we have separately grouped the Givens rotations and the two-body excitations, since the gates with different values of k are mutually commuting. The two-body cluster operator \hat{T} now encodes the rotation angles of the double excitation gates, $t_{pqrs} \in \{0, \frac{\pi}{4}\}$. Then by inserting a resolution of the identity $\hat{F}\hat{F}^\dagger$ we obtain

$$|\Phi\rangle = \hat{G}FF^\dagger \exp(\hat{T} - \hat{T}^\dagger) \hat{F} |x_0\rangle \quad (\text{E8})$$

$$= \hat{G}' \exp(\hat{T}' - \hat{T}'^\dagger) |x_0\rangle, \quad (\text{E9})$$

where

$$\hat{G}' = \hat{G}\hat{F}, \quad \hat{T}' = \hat{F}^\dagger \hat{T} \hat{F}. \quad (\text{E10})$$

The FSWAP network permutes the elements of \hat{T} and may introduce some phase factors of ± 1 , so $t'_{pqrs} \in \{0, \pm \frac{\pi}{4}\}$. If we pre-multiply by another arbitrary orbital rotation, we may absorb this into the definition of \hat{G}' , and thus write

$$\hat{G}|\Phi\rangle = \hat{G}' \exp(\hat{T}' - \hat{T}'^\dagger) |x_0\rangle. \quad (\text{E11})$$

We now extend this result to related UCC ansätze which include double excitations, such as the truncated low-rank factorization of UCCD [69] or the low depth unitary cluster-Jastrow (UCJ) ansatz [7, 70], by showing that they are also able to prepare the fermionic magic states and hence the state $|\Phi\rangle$. In the case of UCJ with a single Jastrow layer [7], the correlated reference state has the form

$$\hat{G}^\dagger \exp(i\hat{J}) \hat{G} |x_0\rangle, \quad (\text{E12})$$

where \hat{J} is a diagonal operator which is a sum over products of pairs of number operators $\hat{n}_p \hat{n}_q$ acting between qubits p and q , with $\hat{n}_p = \hat{a}_p^\dagger \hat{a}_p$ (the low-rank factorization of UCCD truncated to rank $l = 1$ has the same exact form, differing only in how the parameters are computed). As noted in the main text, the CZ gate between qubits p and q is equivalent to $\exp(i\pi\hat{n}_p\hat{n}_q)$, and all diagonal operators commute with each other. One can then prepare the four-qubit state $\frac{1}{2}(|10\rangle + |01\rangle)^{\otimes 2}$ starting from the $|1010\rangle$ state by applying two Givens rotations. Following this, application of three CZ gates in any order yields the magic state $|M\rangle$ defined in Eq. 21. This analysis shows that we can therefore write

$$|\Phi\rangle = \exp(i\hat{J}) \hat{G} |x_0\rangle \quad (\text{E13})$$

for appropriately chosen \hat{G} and \hat{J} . The inverse orbital rotation \hat{G}^\dagger of the UCJ ansatz may then be absorbed into any subsequent orbital rotation that transforms between single-particle bases. This implies that a multi-reference NOQE ansatz with UCJ reference states benefits from the same quantum speedups (classical hardness of strong or weak simulation of the rotated reference states) as a multi-reference NOQE ansatz with UCCD reference states.

Appendix F: Electronic structure concepts

Here we provide a brief overview of some important concepts in electronic structure for the benefit of non-specialists (these are covered comprehensively in Ref. 35). A *molecular orbital*, a.k.a. a *spin-orbital*, is a single-electron function $\omega_p(\vec{r}, \sigma)$, where \vec{r} is a spatial coordinate vector $(x, y, z) \in \mathbb{R}^3$, and σ is a discrete spin coordinate $\in \{\frac{1}{2}, -\frac{1}{2}\}$. *Restricted* and *unrestricted* spin-orbitals are delta-functions in the spin coordinate: restricted spin-orbitals come in pairs consisting of a spin-up and spin-down orbital with the same spatial distribution,

while unrestricted orbitals allow for these to have different spatial distributions. *General* spin-orbitals, on the other hand, can have linear combinations of spin-up and spin-down character within a single orbital. In the following we will assume restricted or unrestricted orbitals, and we will drop the spin coordinate notation, noting that whenever orbitals p and q with opposite spins are integrated over the same set of coordinates the result is zero (i.e., we neglect any spin coupling or fine structure corrections in the Hamiltonian). Molecular orbitals are constructed from linear combinations of primitive basis functions (the *basis set*, e.g., atom-centered Gaussian functions or plane waves) to form an orthonormal set, indexed by $p = 1, \dots, n$:

$$\int_{\vec{r}} \omega_p^*(\vec{r}) \omega_q(\vec{r}) d\vec{r} = \delta_{pq}. \quad (\text{F1})$$

The electronic structure Hamiltonian (Eq. 9) then has one- and two-body coefficients given by

$$h_{pq} = \int_{\vec{r}} \omega_p^*(\vec{r}) \left(-\frac{1}{2} \nabla^2 - \sum_a \frac{Z_a}{\|\vec{r} - \vec{R}_a\|} \right) \omega_q(\vec{r}) d\vec{r}, \quad (\text{F2})$$

$$h_{pqrs} = \int_{\vec{r}, \vec{r}'} \omega_p^*(\vec{r}) \omega_q^*(\vec{r}') \frac{1}{\|\vec{r} - \vec{r}'\|} \omega_r(\vec{r}) \omega_s(\vec{r}') d\vec{r} d\vec{r}', \quad (\text{F3})$$

where a indexes the atomic nuclei with fixed coordinates \vec{R}_a (under the *Born-Oppenheimer* approximation) and atomic charge numbers Z_a , with all quantities expressed in atomic units.

Any sufficiently expressive primitive basis set is *localizable*, meaning that there is an orbital rotation \hat{G} , as defined in the main text, which rotates the basis functions according to

$$\tilde{\omega}_p(\vec{r}) = \sum_q g_{pq} \omega_q(\vec{r}), \quad (\text{F4})$$

such that the rotated functions $\tilde{\omega}_p$ are largely confined to certain regions of space and decay rapidly outside of these regions. In the case of atom-centered Gaussian primitives, $\tilde{\omega}_p$ might correspond to a linear combination of atomic orbitals around a single atomic center, while in the case of plane wave primitives, $\tilde{\omega}_p$ may correspond to a wavepacket with a compact envelope. When the orbitals are spatially localized, the rotated Hamiltonian coefficients \tilde{h}_{pq} and \tilde{h}_{pqrs} (obtained by Eqs. F2, F3 substituting ω_p with $\tilde{\omega}_p$, etc.) are largest for interactions between MOs confined to neighboring spatial regions, and decay with increasing separation following the $1/r$ dependence of the Coulomb potential. This illustrates the importance of the molecular orbital basis in quantum chemistry, which can significantly affect the computational hardness of the electronic structure problem.

A *Slater determinant* is a multi-electron wavefunction describing uncorrelated indistinguishable fermions, constructed so as to respect wavefunction antisymmetry under exchange of any pair of particle coordinates. Let

$\omega_1, \dots, \omega_\eta$ be a set of occupied MOs. Then the corresponding η -particle Slater determinant Ω is given by

$$\Omega(\vec{r}_1, \dots, \vec{r}_\eta) = \frac{1}{\sqrt{\eta!}} \begin{vmatrix} \omega_1(\vec{r}_1) & \cdots & \omega_\eta(\vec{r}_1) \\ \vdots & \ddots & \vdots \\ \omega_1(\vec{r}_\eta) & \cdots & \omega_\eta(\vec{r}_\eta) \end{vmatrix}, \quad (\text{F5})$$

where $|\cdot|$ indicates the matrix determinant operation, and the ‘matrix elements’ are single-particle wavefunctions. The result is a sum over all products of the occupied orbitals with permuted particle coordinates, multiplied by a sign of ± 1 according to the parity of the permutation. In the Fock space representation, each Fock space vector $|x\rangle = |x_1 \dots x_n\rangle$, where $x_p = 1$ if ω_p is occupied or 0 otherwise, corresponds to a unique Slater determinant Ω_x . The *Hartree-Fock* (HF) self-consistent field method is used to find the set of molecular orbitals that give rise to the lowest energy η -electron Slater determinant. We denote this by $|x_0\rangle$, to indicate that the orbitals are filled in order of increasing energy, so the HF method finds the optimal set of occupied molecular orbitals $\{\omega_p\}_{p=1}^\eta$, as linear combinations of the primitive basis set, in order to minimize $\langle x_0 | \hat{H} | x_0 \rangle$. This algorithm can be constrained to optimize over spin-restricted orbitals (RHF) or unrestricted orbitals (UHF).

Configuration interaction (CI) refers to diagonalization in a basis of Slater determinants. For example, the lowest energy vector in the complete basis of η -electron Slater determinants provides the full configuration interaction (FCI) wavefunction,

$$|\Psi_{\text{FCI}}\rangle = \sum_x c_x |x\rangle, \quad (\text{F6})$$

where x runs over all computational basis vectors with the correct particle number (and total z -spin component). Within the non-relativistic quantum theory, and under the Born-Oppenheimer and finite basis approximations, this provides the exact ground state energy,

$$\langle \Psi_{\text{FCI}} | \hat{H} | \Psi_{\text{FCI}} \rangle = E_0. \quad (\text{F7})$$

Because diagonalizing over all $\binom{n}{\eta}$ basis vectors is computationally intractable, an efficiently representable *ansatz* state $|\psi\rangle$ is chosen to approximate this wavefunction. Any normalized vector in the Fock space satisfies the *variational principle*. this means that if $|\psi\rangle$ can be reliably and efficiently normalized, then $\langle \psi | \hat{H} | \psi \rangle \geq E_0$ can be guaranteed. This is an important property for the design of reliable quantum chemistry methods to minimize the expected energy, as the obtained estimate then never goes below the true value.

Another desired property of $|\psi\rangle$ is *size-consistency*. Consider two spatially separated molecular fragments A and B . Using sets of localized MOs confined to each fragment, in the limit of $r_{AB} \rightarrow \infty$ we may write

$$\hat{H}_{AB} = \hat{H}_A \otimes \hat{\mathbb{1}}_B + \hat{\mathbb{1}}_A \otimes \hat{H}_B. \quad (\text{F8})$$

Suppose that a classical or quantum algorithm, when applied separately to subsystems A and B , produces ansatz states $|\psi_A\rangle$ with energy estimate E_A and $|\psi_B\rangle$ with estimate E_B . If the method is size-consistent, then when applied to the composite system described by Eq. F8 it should produce the energy estimate $E_{AB} = E_A + E_B$, corresponding to the product wavefunction $|\psi_A\rangle \otimes |\psi_B\rangle$. Simply put, increasing the size of the system should not reduce the accuracy of the ansatz within each fragment.

Correlated electronic wavefunctions are categorized using loose descriptors for different types of electronic correlation. Broadly speaking, *dynamic correlation* (also known as *weak correlation*, not to be confused with dynamical evolution) refers to many small contributions from highly excited determinants. For example, consider a coupled-cluster doubles (CCD) wavefunction,

$$|\psi_{\text{CCD}}\rangle = \exp(\hat{T}) |x_0\rangle = \sum_{k=0}^{\infty} \frac{1}{k!} \hat{T}^k |x_0\rangle, \quad (\text{F9})$$

where the two-body excitation generator \hat{T} is defined as in Eq. 28, with $|t_{pqrs}| \ll 1$ (by which we mean that the largest double excitation amplitude is smaller than unity in absolute value by at least roughly an order of magnitude). This wavefunction is dominated by a single determinant, $|x_0\rangle$, with small contributions from many excited determinants which decay with increasing excitation order (here parameterized by k). This can be thought of as a perturbative correction to the *reference state* $|x_0\rangle$. *Static correlation*, on the other hand, generally refers to the non-perturbative features of the electronic wavefunction, which must be described using multiple reference states of large amplitude (also known as *strong correlation*). For example, a wavefunction exhibiting a moderate amount of static correlation, but with little dynamic correlation, might be well described by a configuration interaction ansatz obtained by diagonalizing in the subspace of $O(n^4)$ doubly excited determinants (CID),

$$|\psi_{\text{CID}}\rangle = \sum_{pqrs}^n c_{pqrs} \hat{a}_p^\dagger \hat{a}_q^\dagger \hat{a}_r \hat{a}_s |x_0\rangle. \quad (\text{F10})$$

Alternatively, the non-orthogonal configuration interaction (NOCI) ansatz may be applicable to model such a system, which takes the form of Eq. 23, where the reference states are single Slater determinants in rotated orbital bases (for instance, these could be chosen as degenerate UHF solutions [50]). In the main text we have expanded this notion of a reference state from a single Slater determinant to include compact correlated states in different orbital bases, in particular MPS or UCCD states, enabling far more flexible treatment of both types of electronic correlation. We stress that the line between static and dynamic correlation is not precise, and their features are emphasized differently depending on the context [46–48].

Note that the CCD wavefunction in Eq. F9 is size-consistent but is not variational (the same is true for CCSD and CCSD(T), regarded as the “gold standard” of quantum chemistry). On the other hand, the CID wavefunction in Eq. F10 is variational but is not size-consistent. Developing a computationally tractable wavefunction ansatz which is both variational and size-consistent, and which faithfully represents ground state wavefunctions exhibiting both static and dynamic electronic correlation, is the essential challenge of ground state quantum chemistry [46]. The quantum subspace framework of TNQE and NOQE ensures strict variationality in the obtained energy estimate, and in both cases the reference states are size-consistent, which enables the multi-reference ansatz to recover size-consistency in the limit of increasing subspace dimension (i.e., a sufficient number of reference states, M). The scaling of M with the system size in order to achieve a constant additive error in the energy estimate will be system dependent, and the overall cost in terms of classical and quantum computational resources may be benchmarked against other hybrid quantum-classical approaches. Empirical studies have so far suggested highly favorable performance and resource estimates versus comparable quantum and classical methods [7, 8].